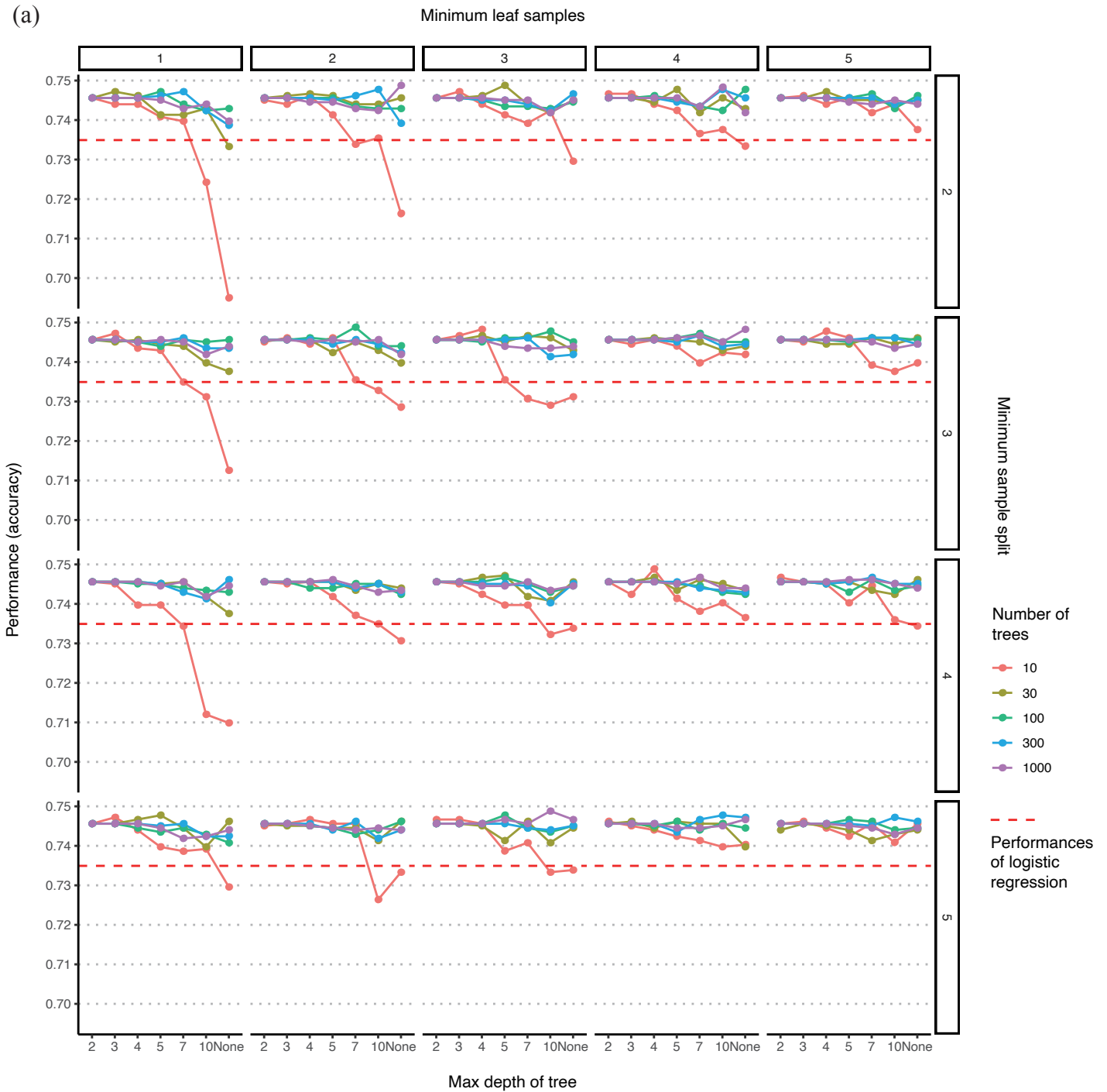
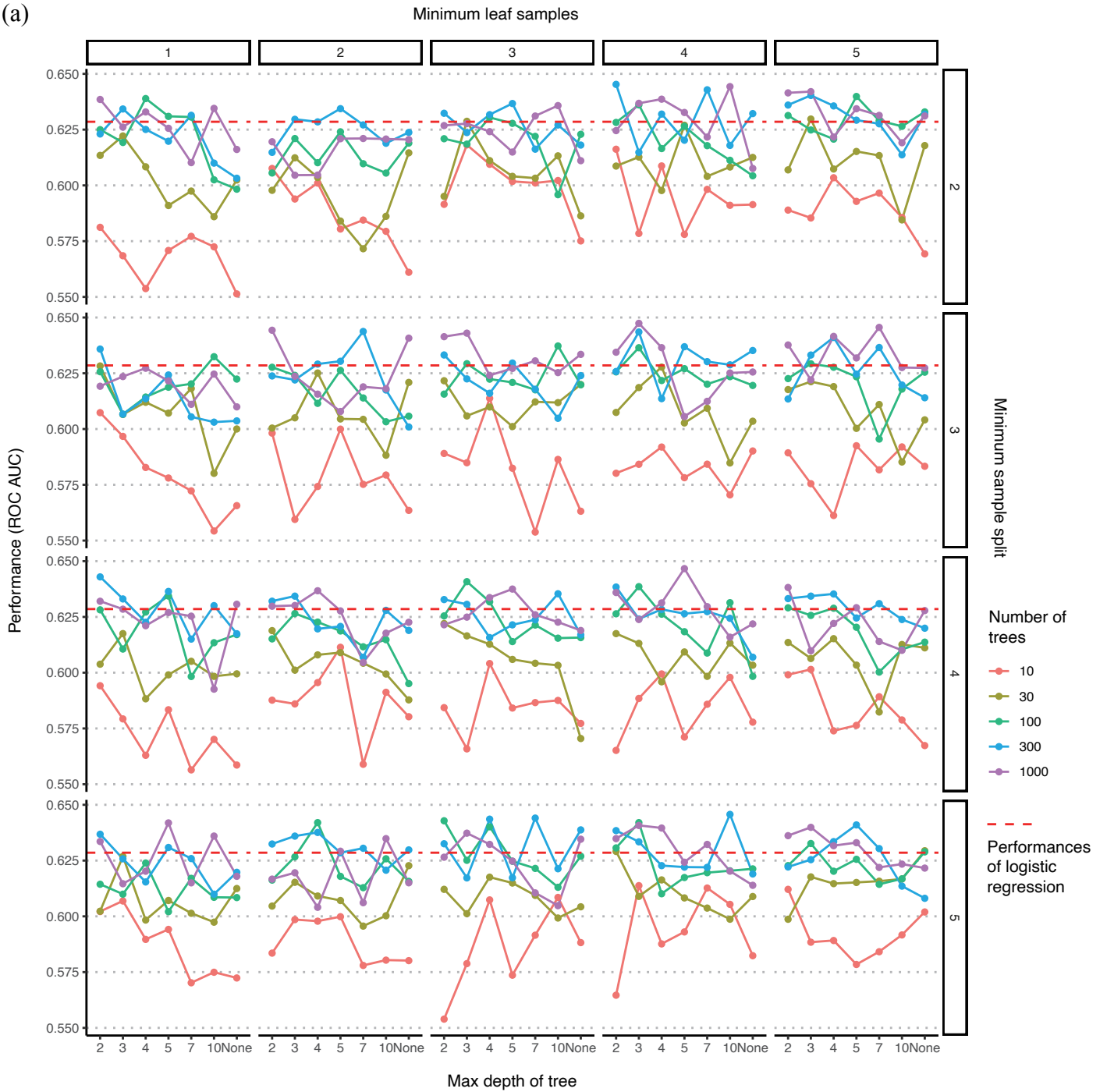
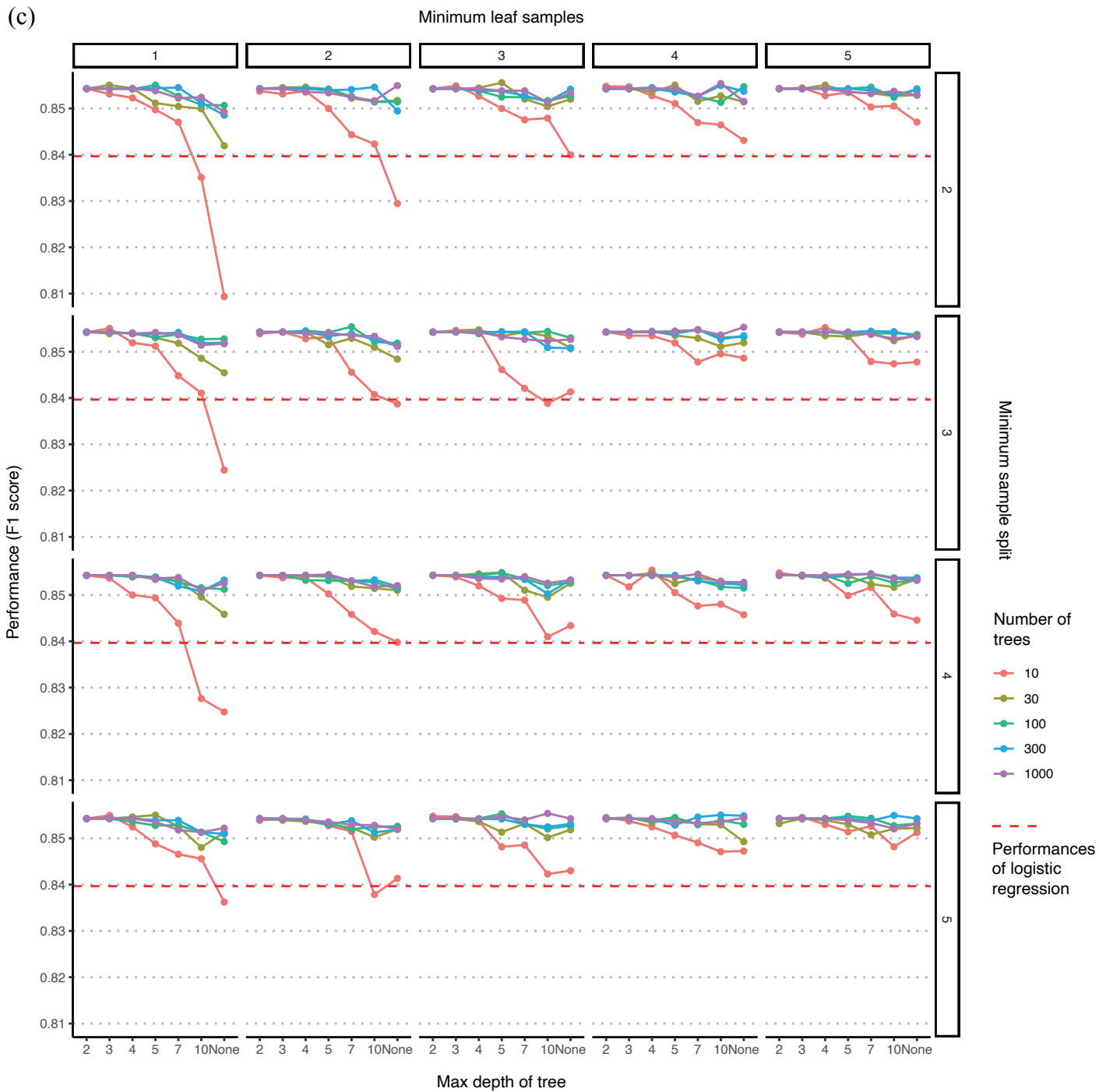


Figure S1. Prediction performances of RF-method model by varying maximum depths of a tree, numbers of trees, minimum sample split, and minimum leaf samples in patients with RA. The X-axis represents the differing maximum depths of a decision tree. The Y-axis represents the (a) accuracy, (b) AUC of the ROC curve, (c) F1 score, and (d) AUC of the precision-recall curve. The performances of the models based on the numbers of trees are depicted as a line. The dashed red horizontal lines represent the prediction performance of logistic regression models.



(a)





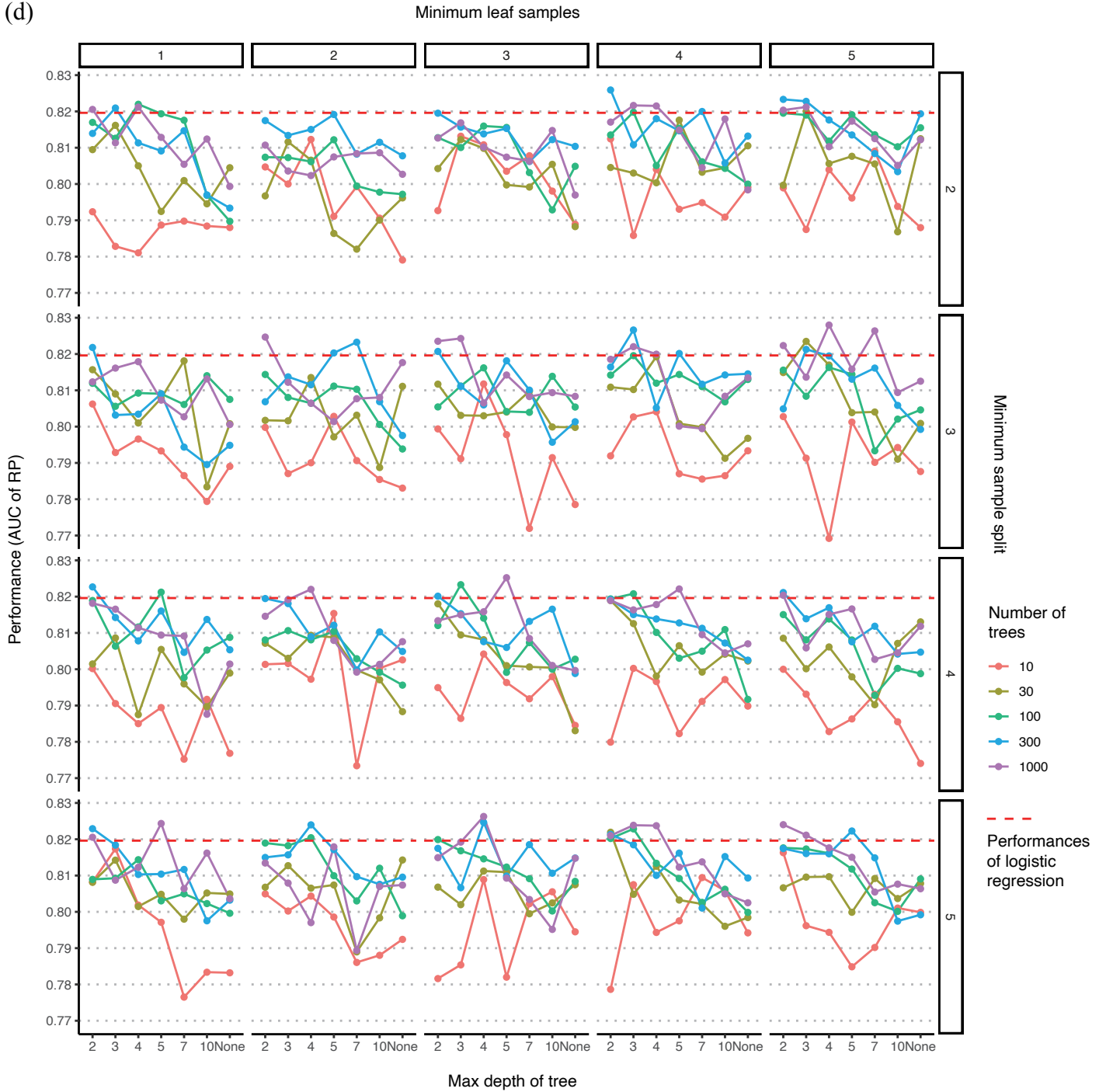
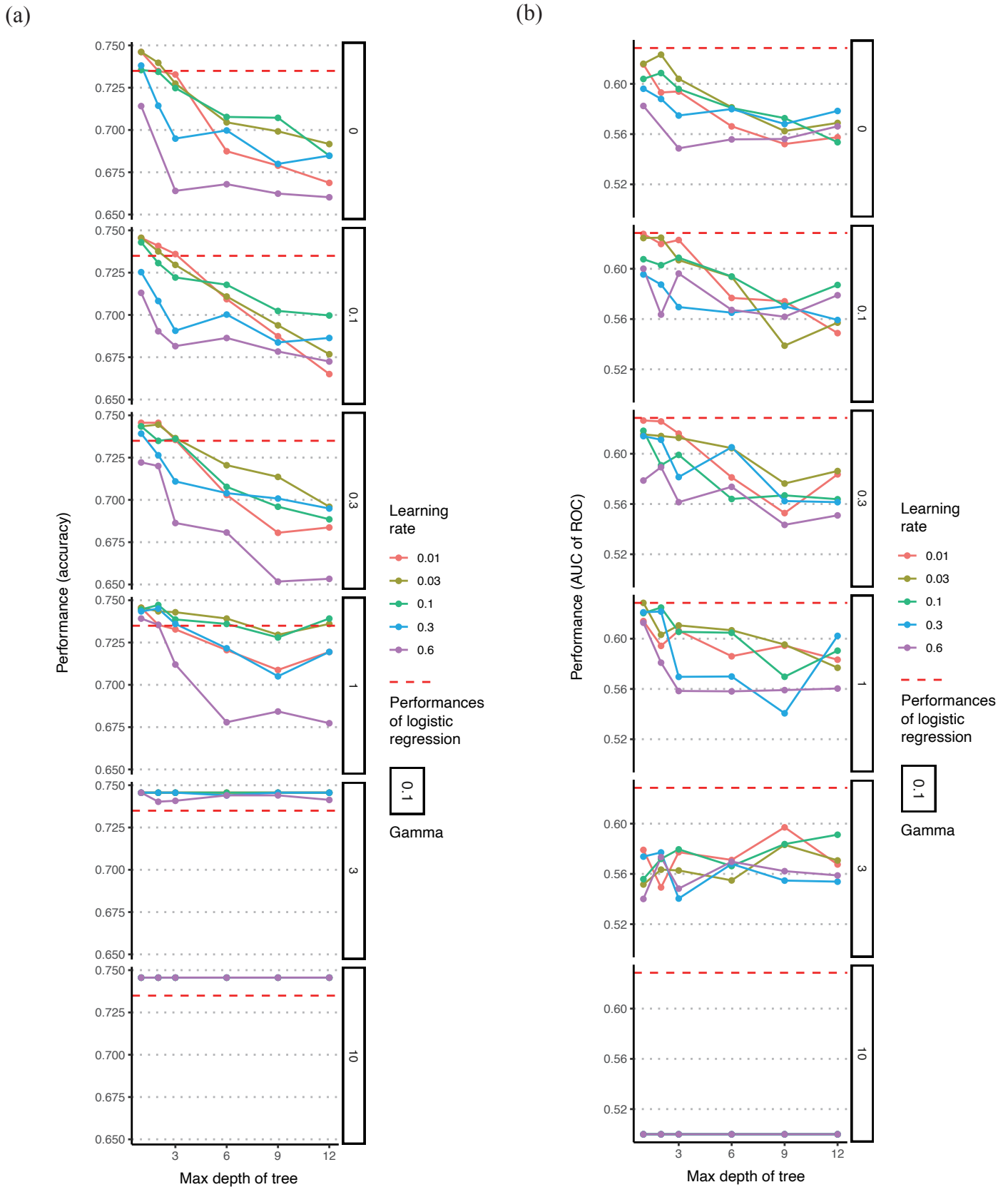
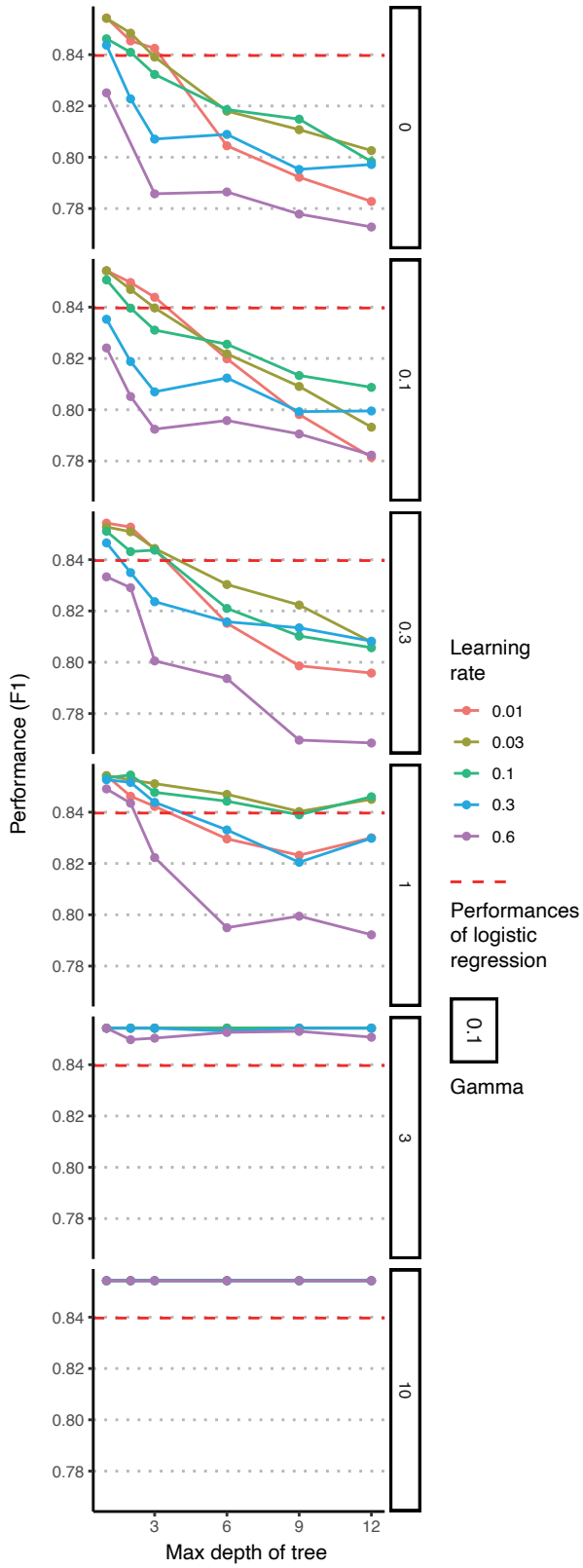


Figure S2. Prediction performances of XGBoost model by varying maximum depths of a tree and numbers of trees in patients with RA. The X-axis represents the differing maximum depths of a decision tree. The Y-axis represents the (a) accuracy, (b) AUC of the ROC curve, (c) F1 score, and (d) AUC of the precision-recall curve. The performances of the models based on the numbers of trees are depicted as a line. The dashed red horizontal lines represent the prediction performance of logistic regression models.



(c)



(d)

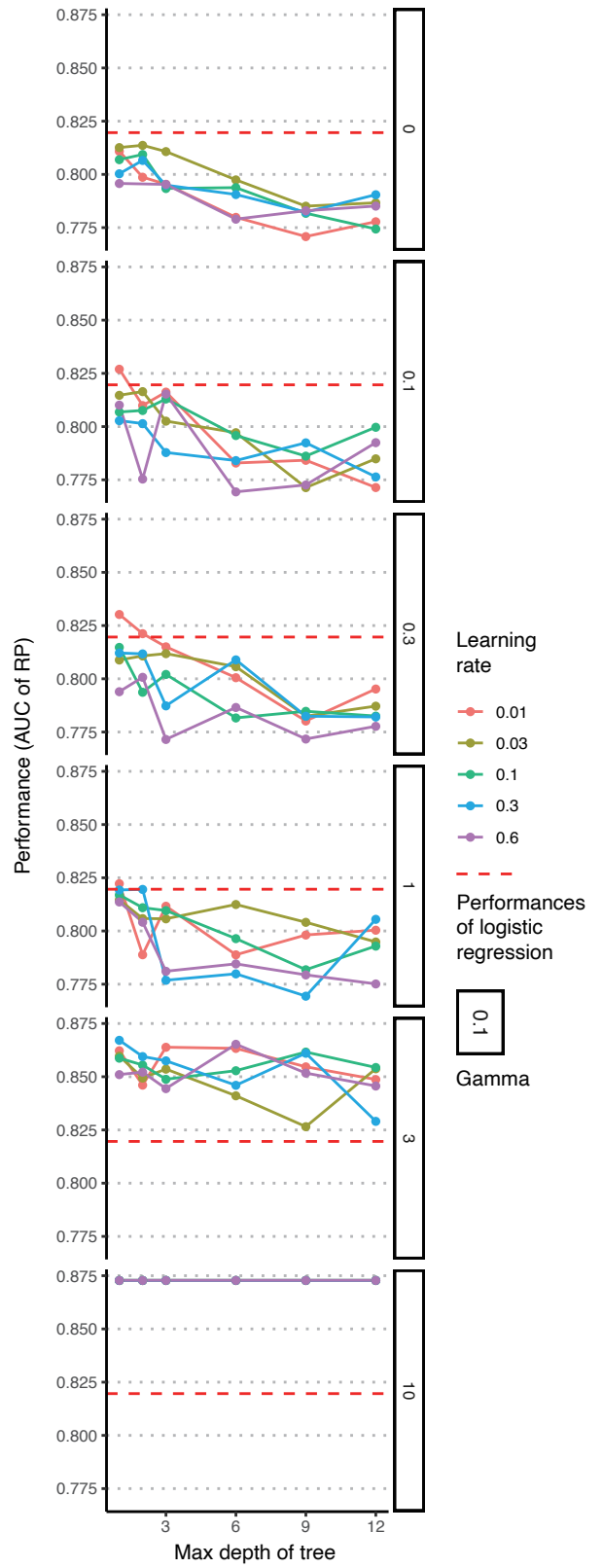
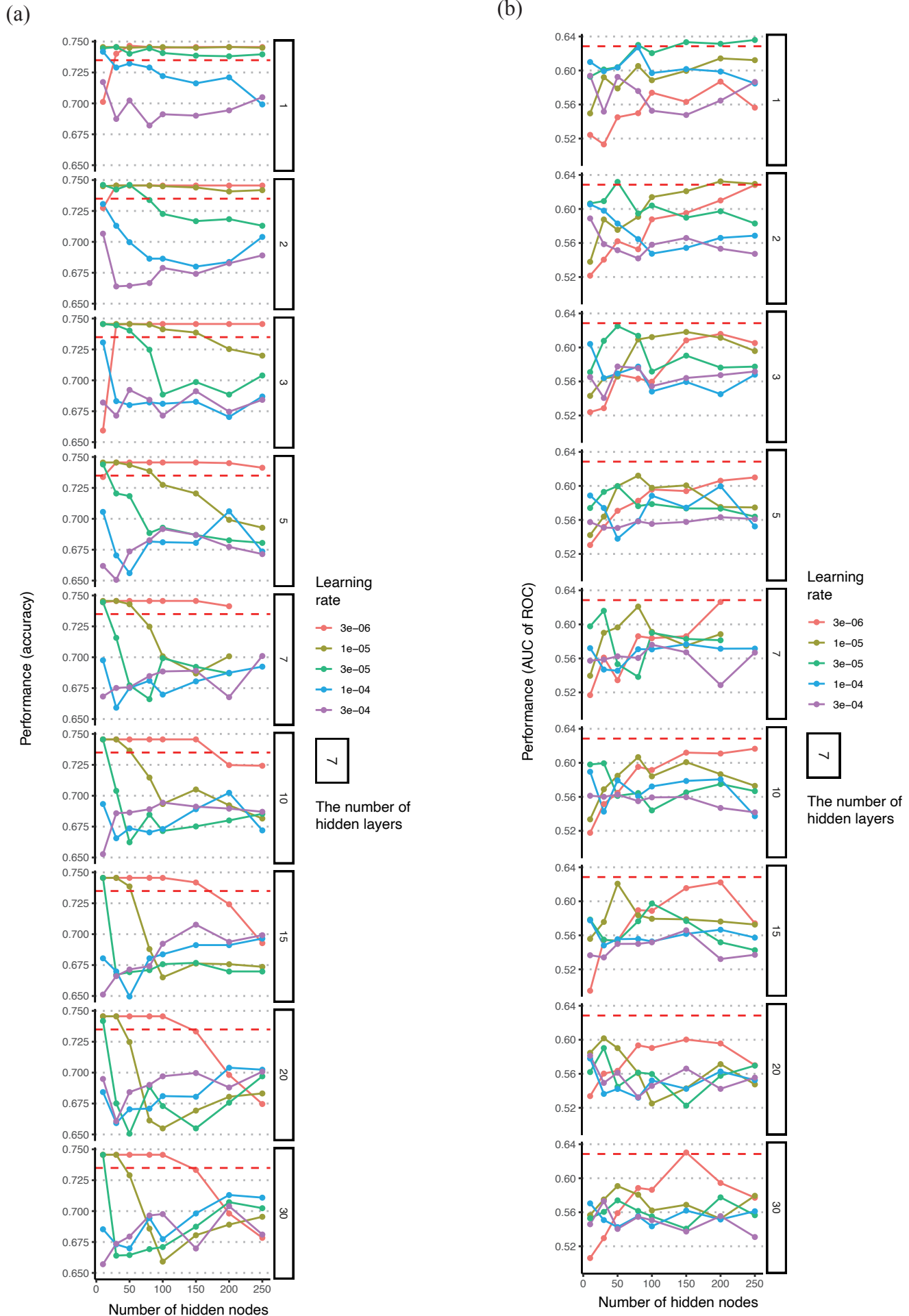
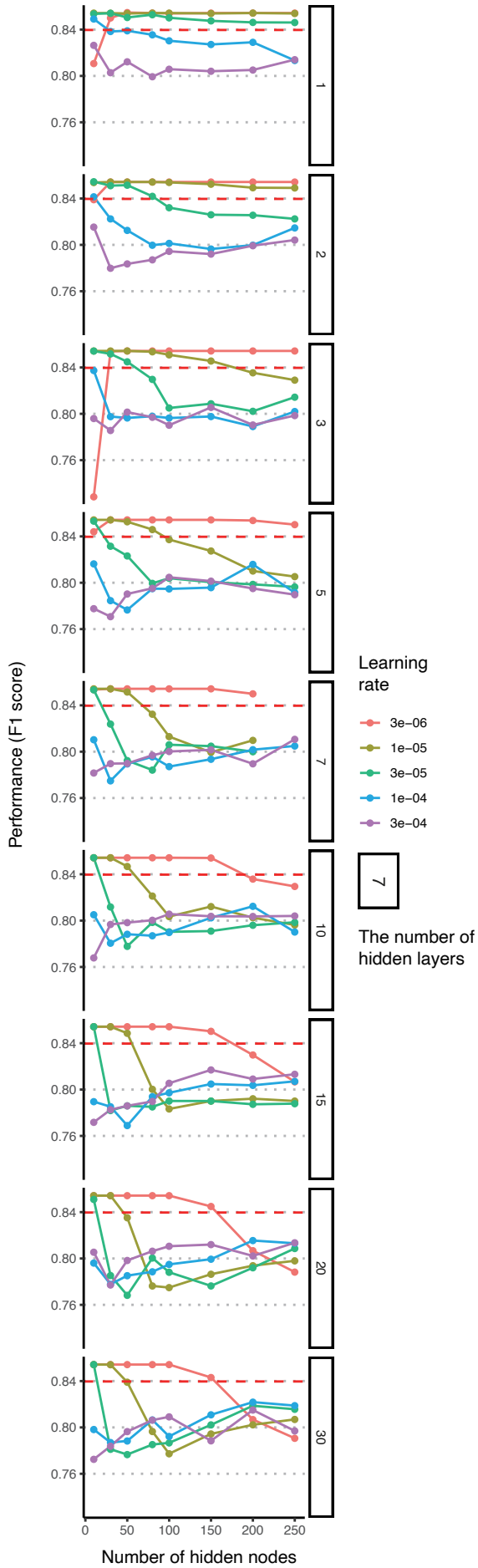


Figure S3. Prediction performances of ANN with varying numbers of hidden layers, hidden nodes, and learning rates in patients with RA. The X-axis represents the differing numbers of hidden nodes of each hidden layer. The Y-axis represents the (a) accuracy, (b) AUC of the ROC curve, (c) F1 score, and (d) AUC of the precision-recall curve. The performances of the models from each learning rate are depicted as a line. The dashed red horizontal lines represent the prediction performance of logistic regression models.



(c)



(d)

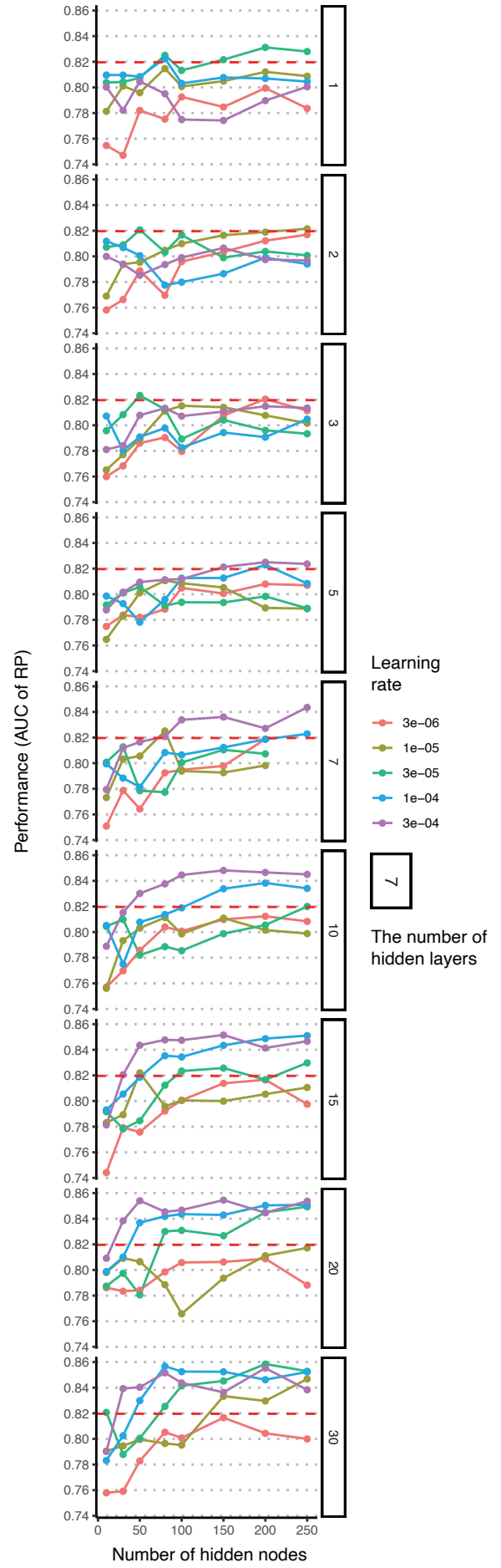
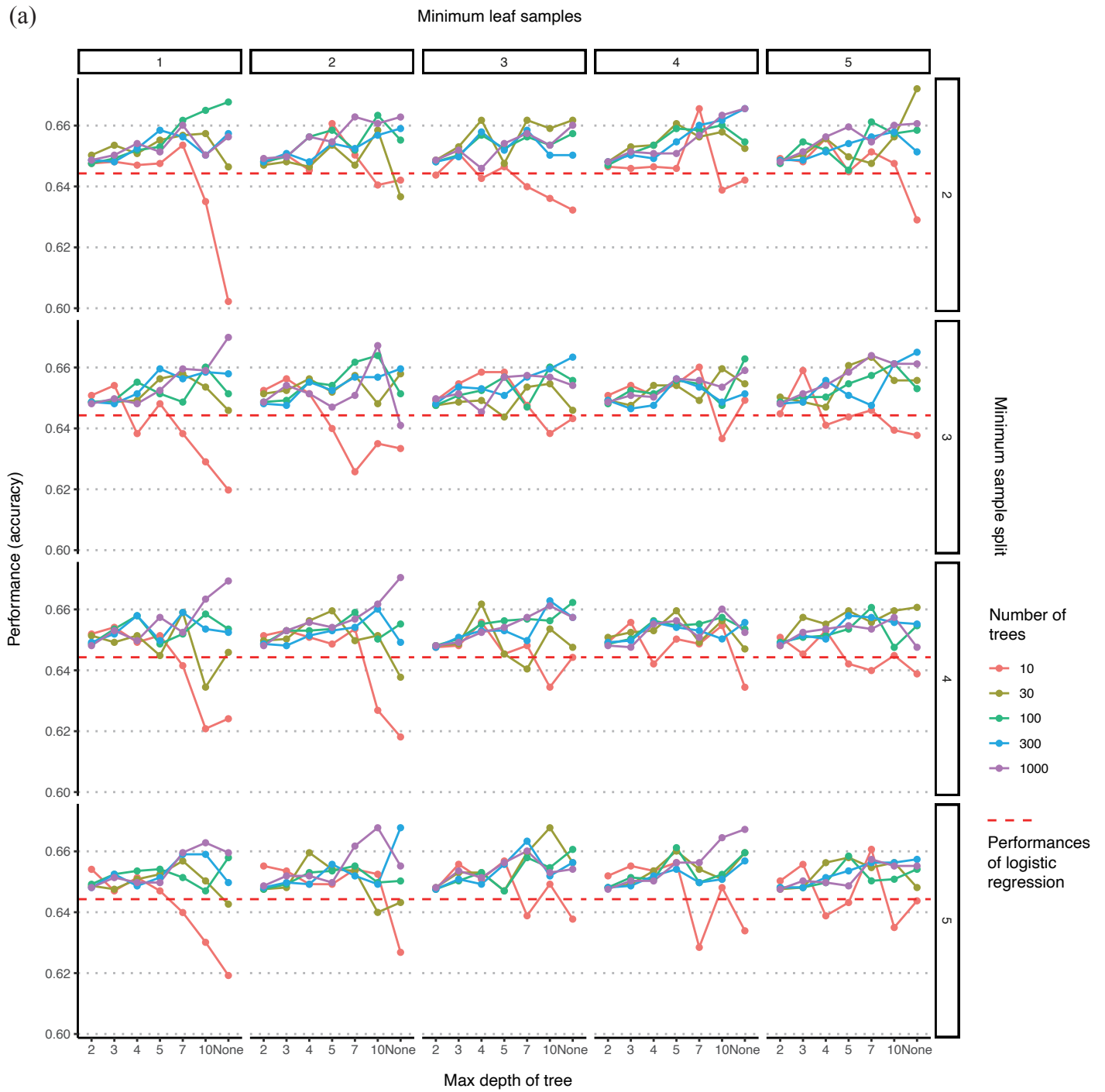
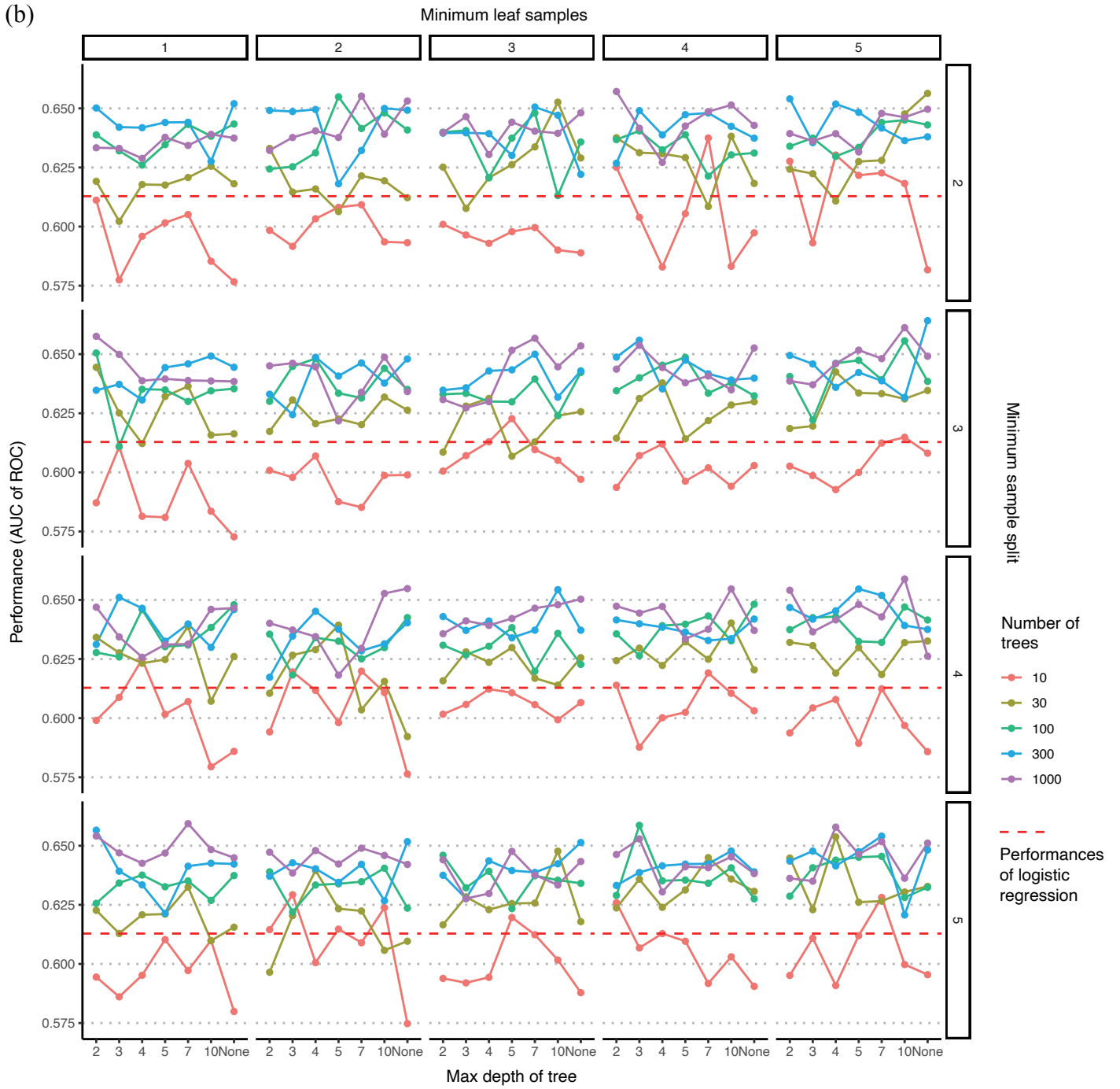
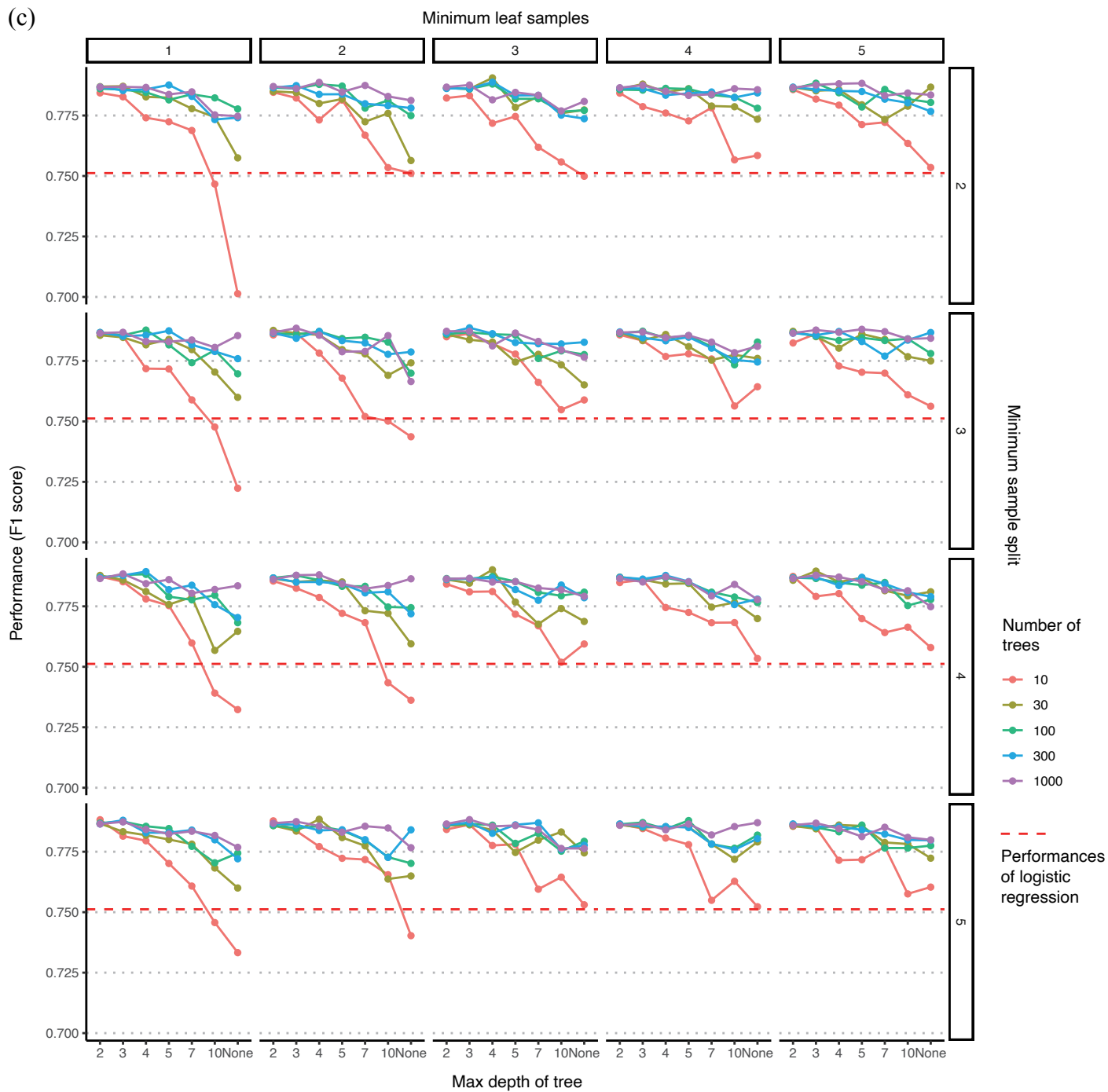


Figure S4. Prediction performances of RF-method model by varying maximum depths of a tree, numbers of trees, minimum sample split, and minimum leaf samples in patients with AS. The X-axis represents the differing maximum depths of a decision tree. The Y-axis represents the (a) accuracy, (b) AUC of the ROC curve, (c) F1 score, and (d) AUC of the precision-recall curve. The performances of the models based on the numbers of trees are depicted as a line. The dashed red horizontal lines represent the prediction performance of logistic regression models.





(c)



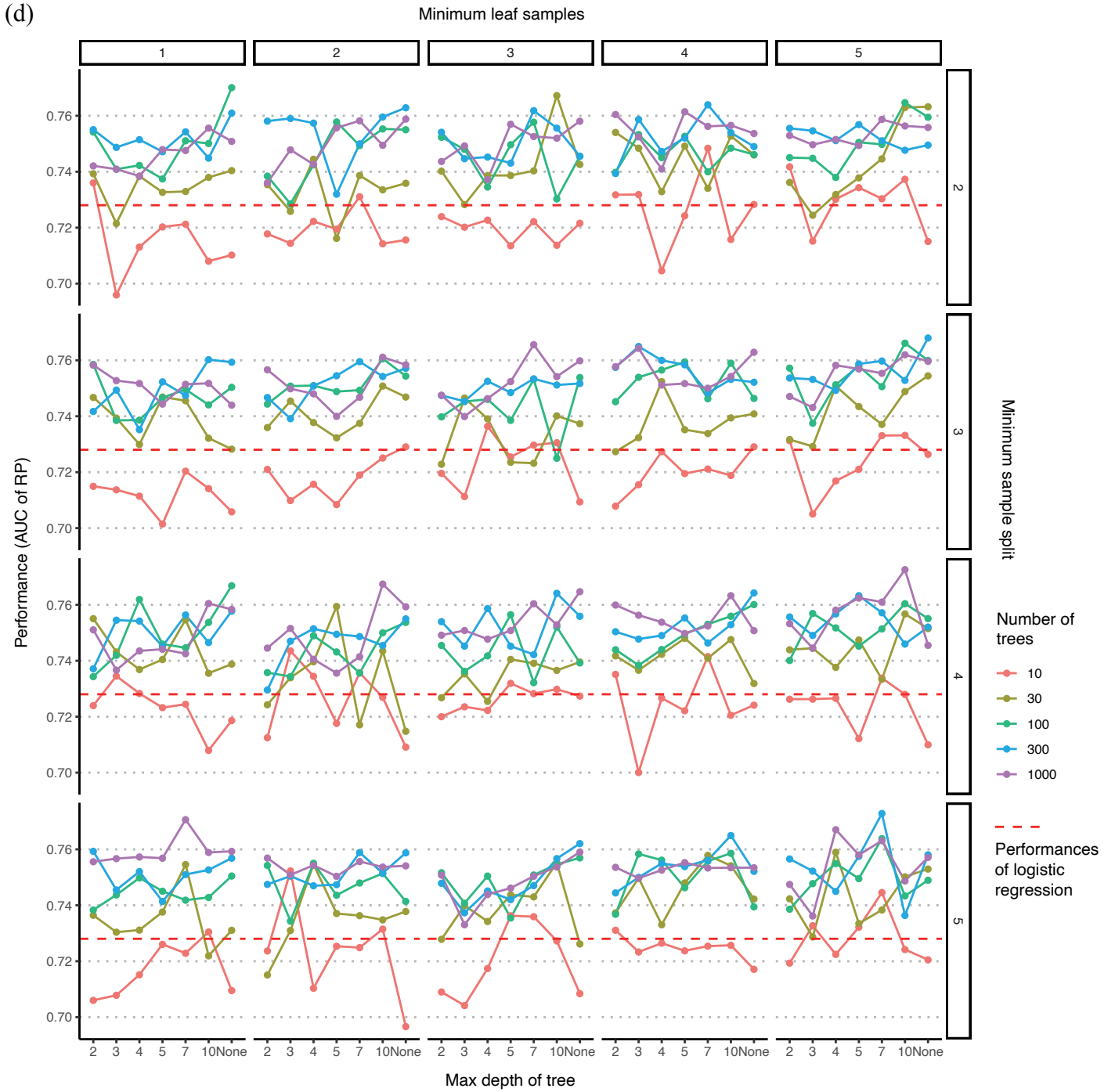
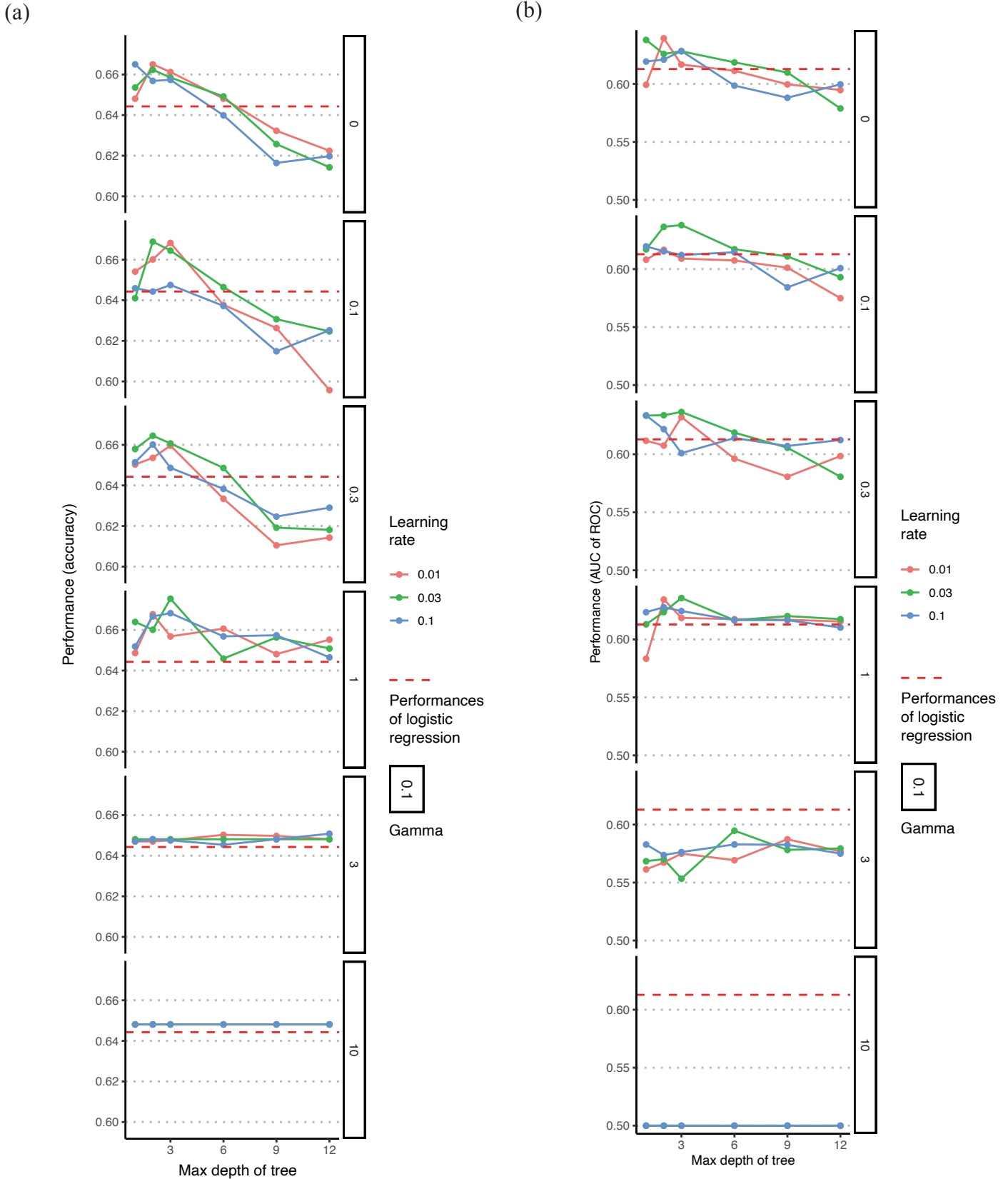
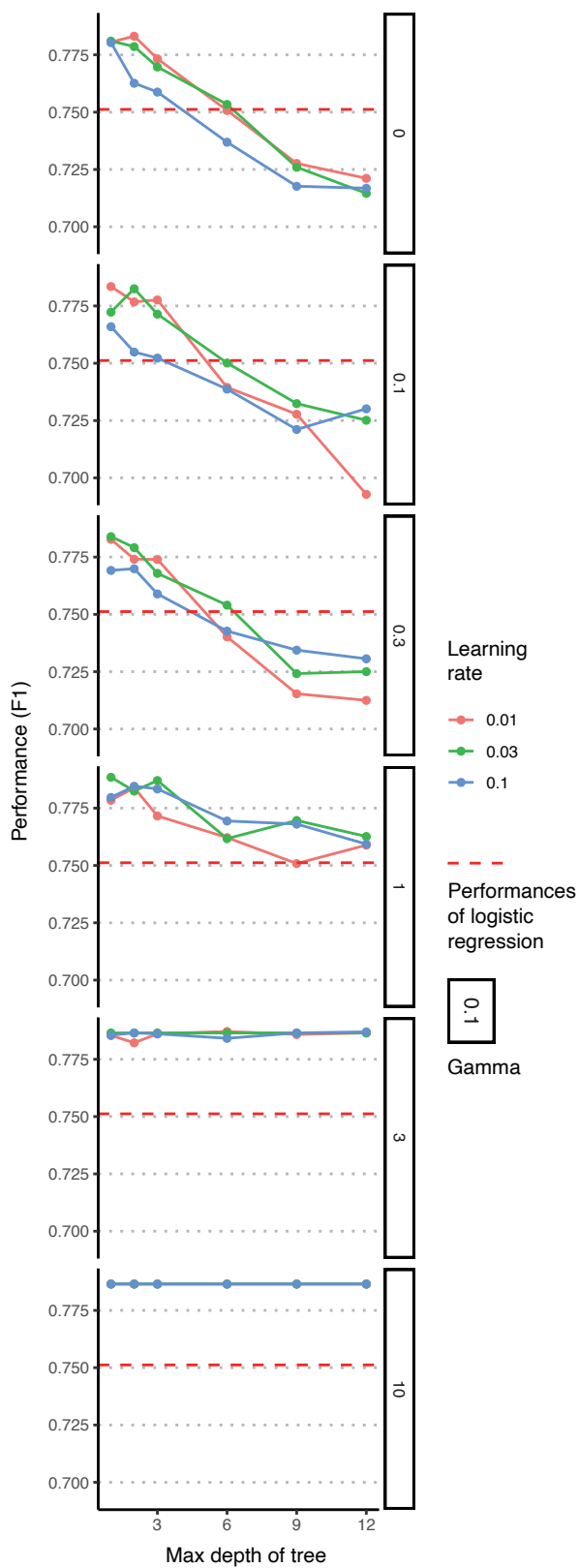


Figure S5. Prediction performances of XGBoost model by varying maximum depths of a tree and numbers of trees in patients with AS. The X-axis represents the differing maximum depths of a decision tree. The Y-axis represents the (a) accuracy, (b) AUC of the ROC curve, (c) F1 score, and (d) AUC of the precision-recall curve. The performances of the models based on the numbers of trees are depicted as a line. The dashed red horizontal lines represent the prediction performance of logistic regression models.



(c)



(d)

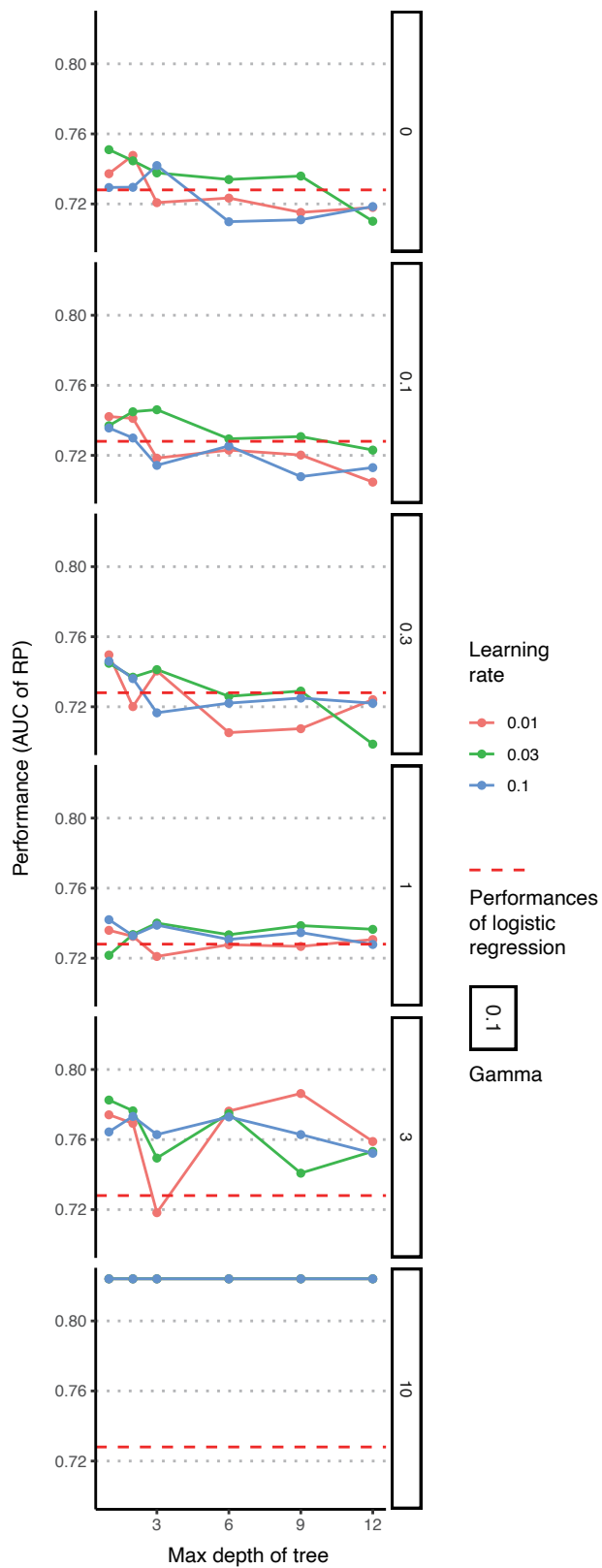
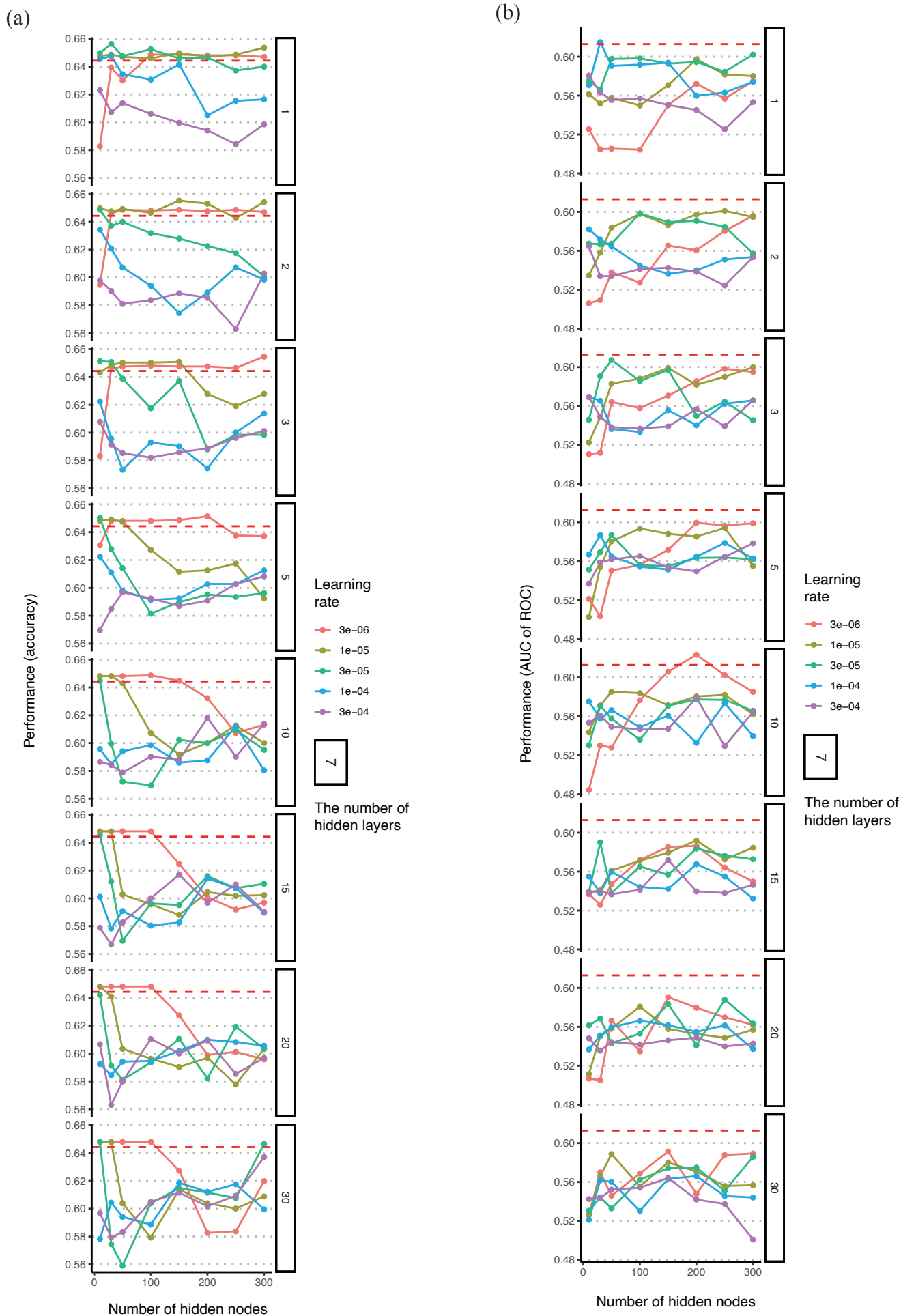
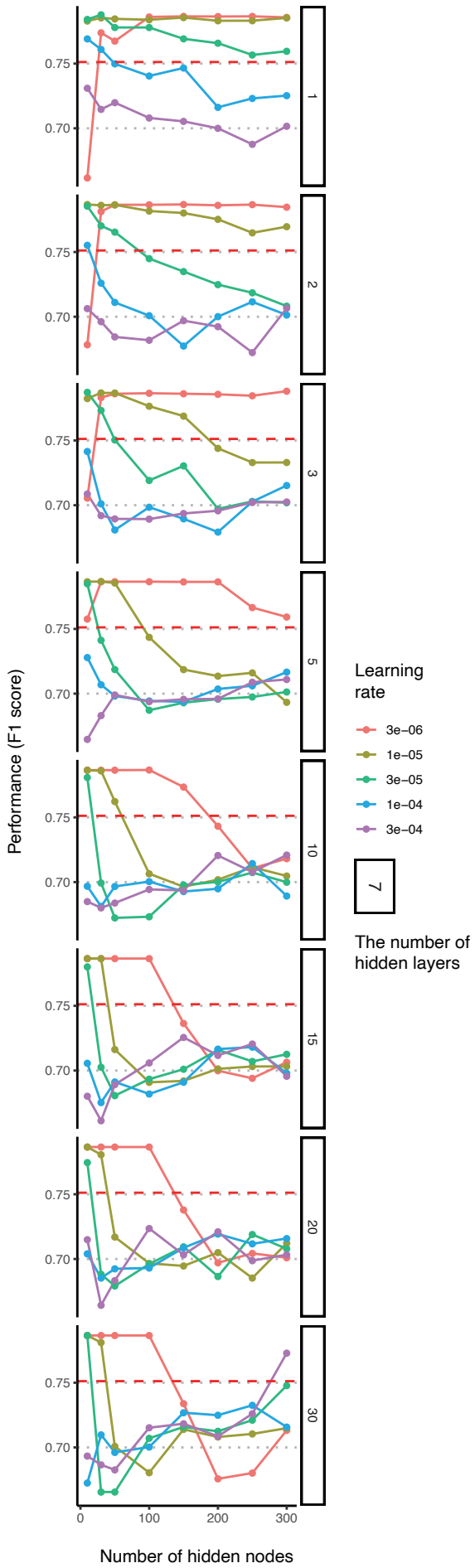


Figure S6. Prediction performances of ANN with varying numbers of hidden layers, hidden nodes, and learning rates in patients with AS. The X-axis represents the differing numbers of hidden nodes of each hidden layer. The Y-axis presents the (a) accuracy, (b) AUC of the ROC curve, (c) F1 score, and (d) AUC of the precision-recall curve. The performances of the models from each learning rate are depicted as a line. The dashed red horizontal lines represent the prediction performance of logistic regression models.



(c)



(d)

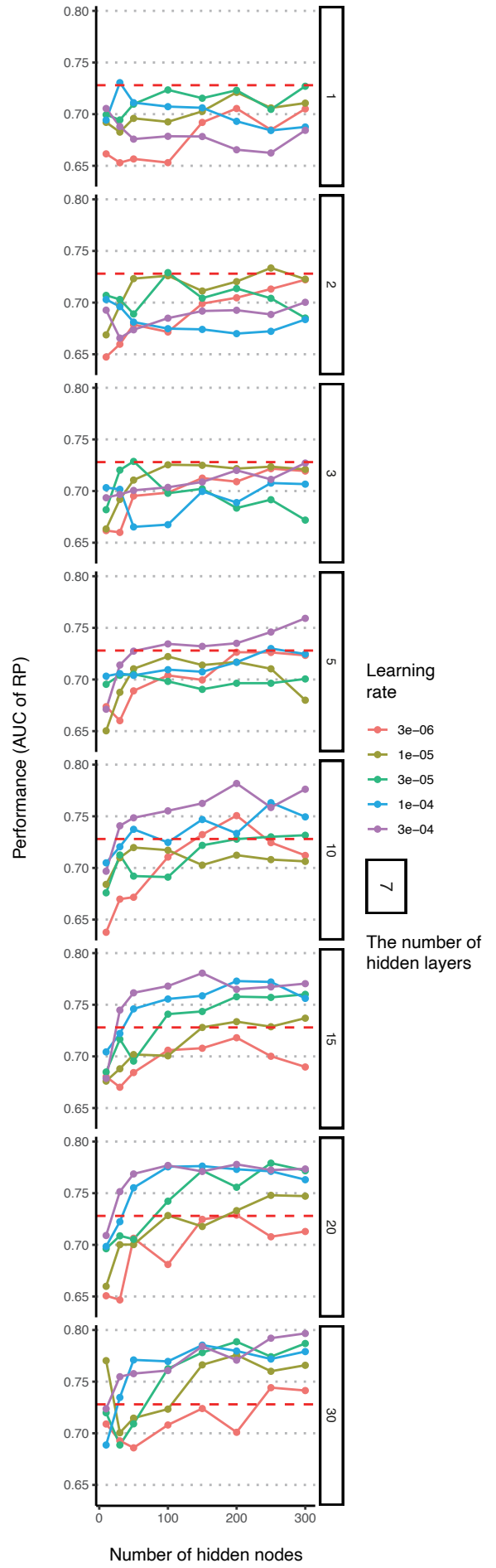
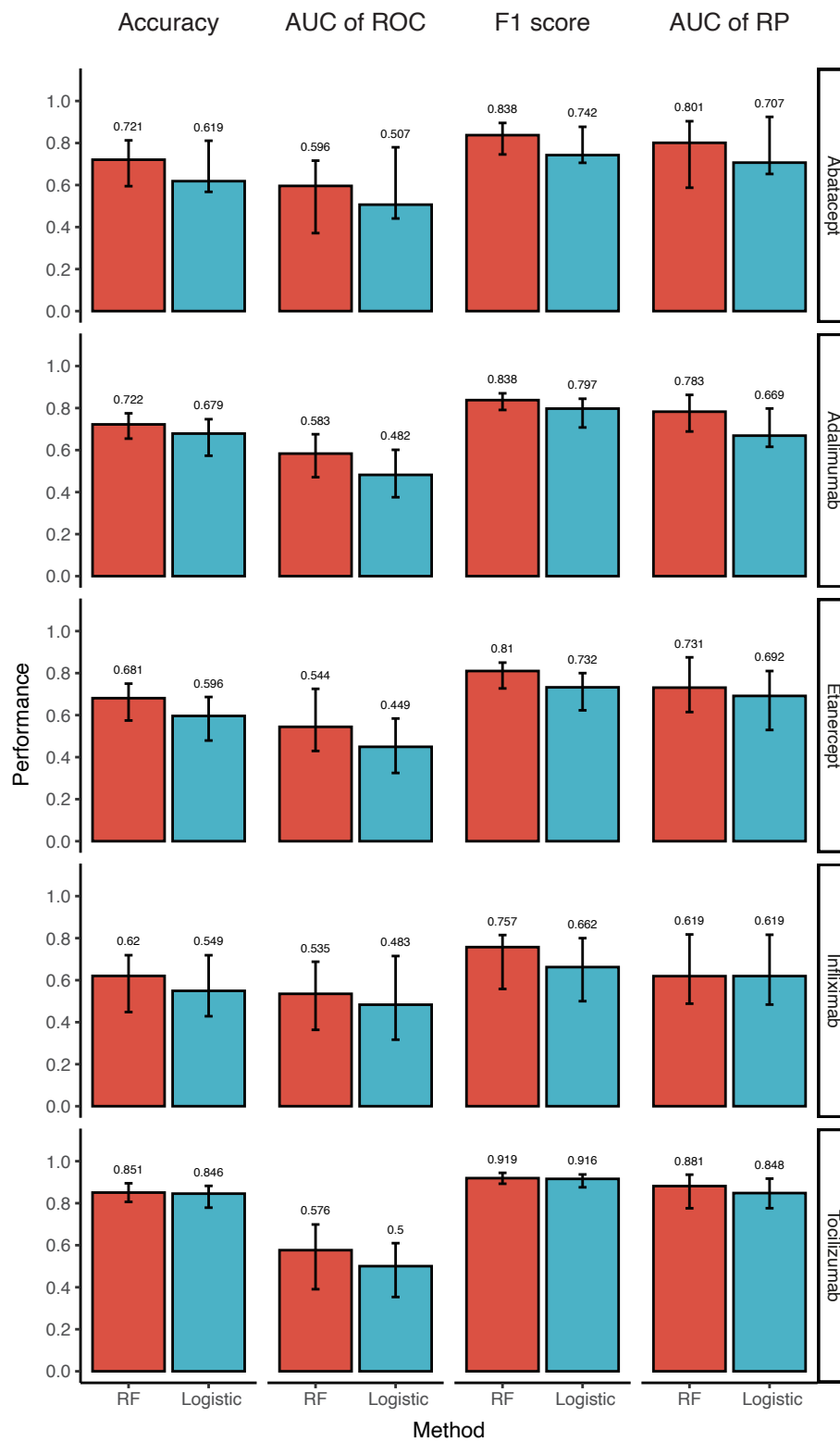


Figure S7. Performance of RF-method and logistic regression models in RA patients divided by the type of bDMARDs, (a) by training dataset, and (b) by independent test dataset.

(a)



(b)

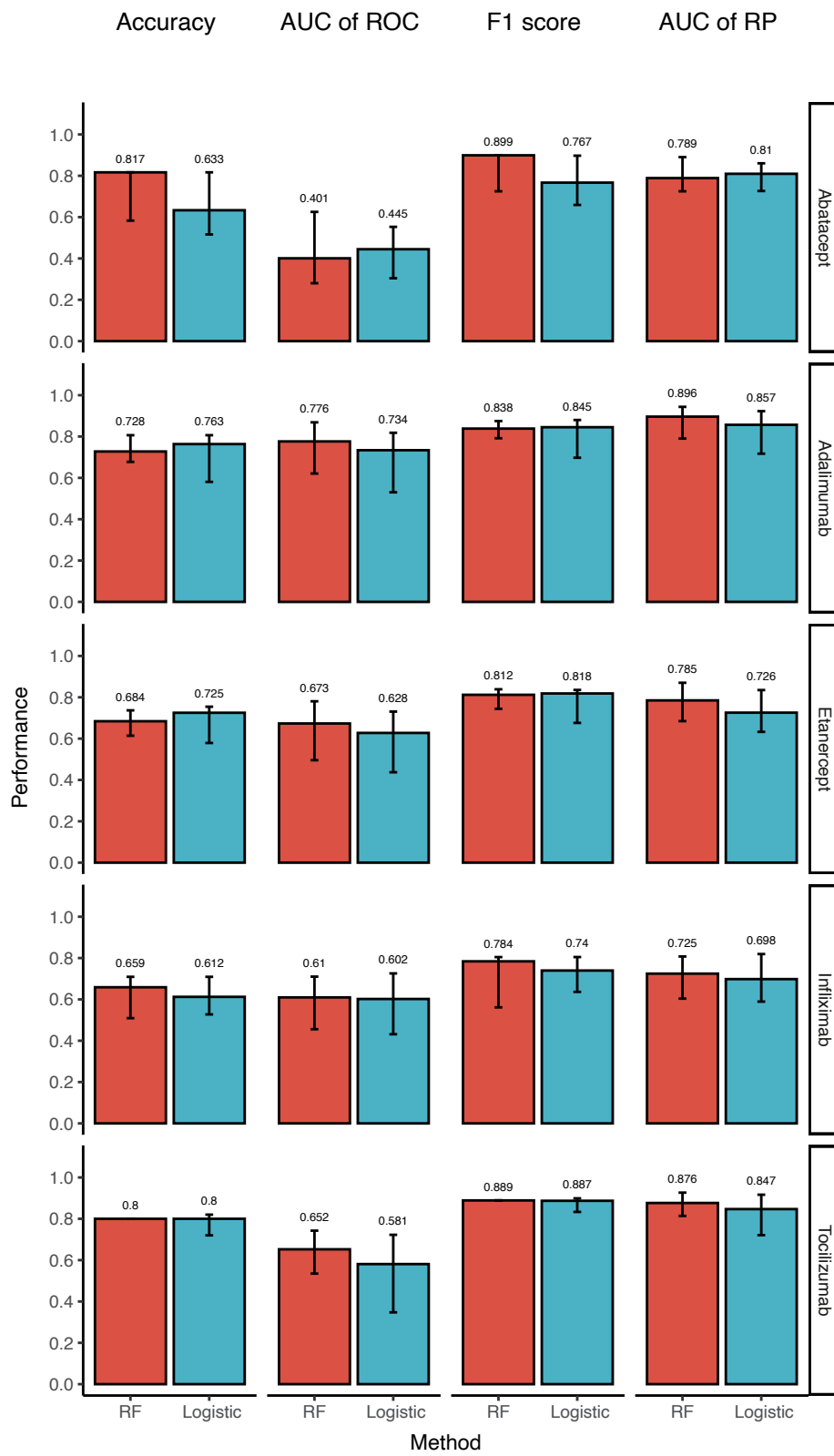
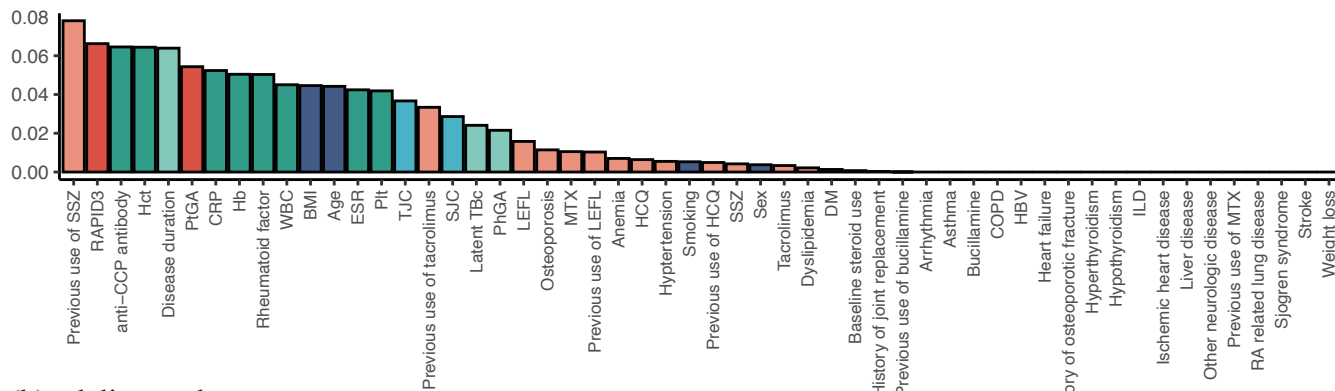
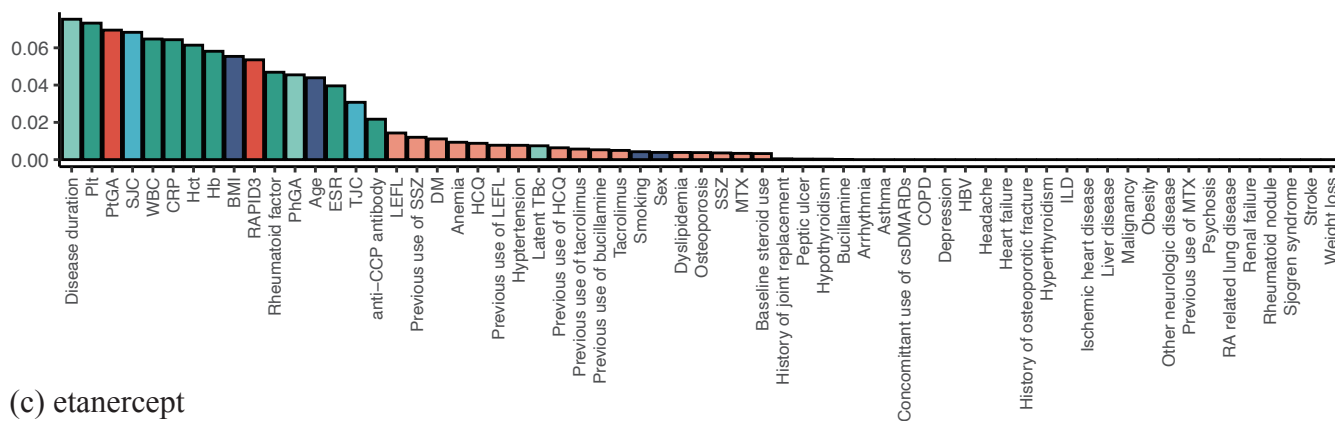


Figure S8. Result of the feature importance analysis of the best-performing RF-method model in RA patients divided by the type of bDMARDs. (a) Abatacept, (b) adalimumab, (c) etanercept, (d) infliximab, and (e) tocilizumab.

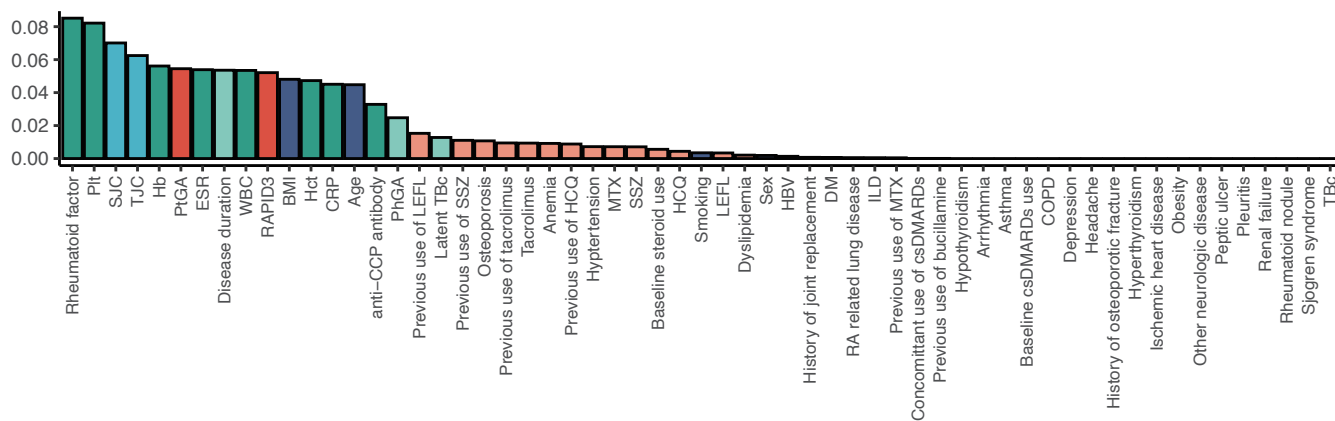
(a) abatacept



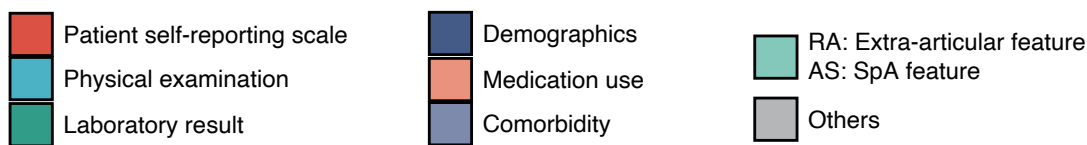
(b) adalimumab



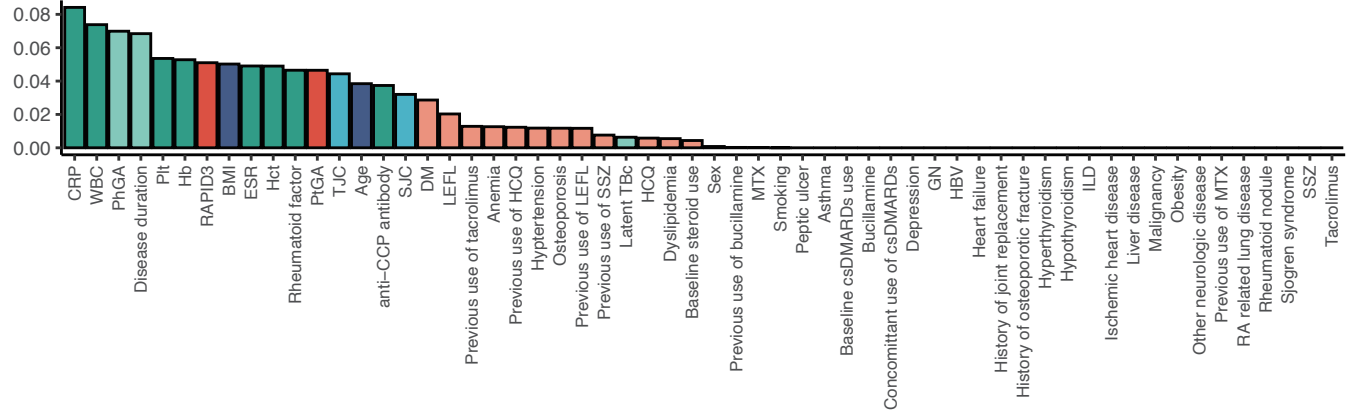
(c) etanercept



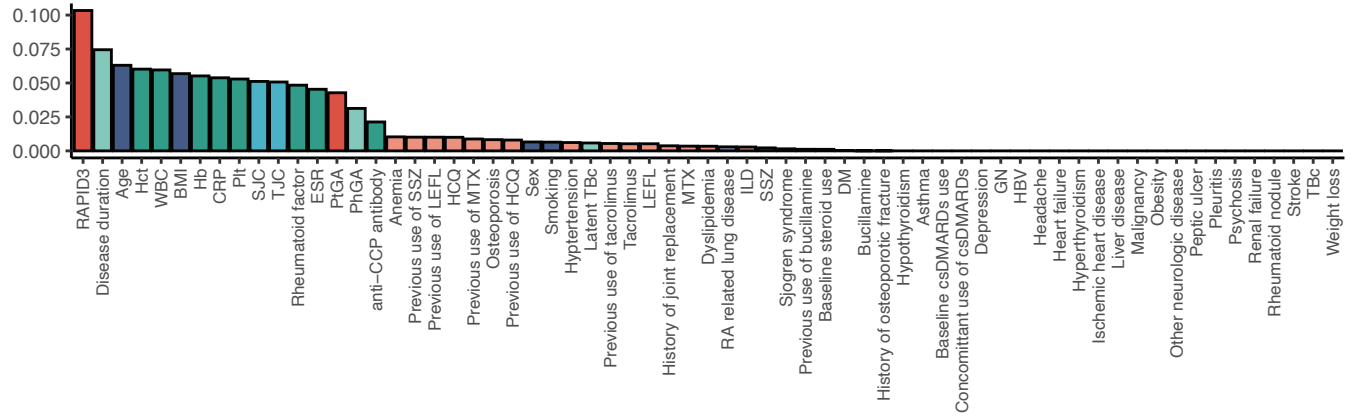
Category



(d) etanercept



(e) tocilizumab



Category

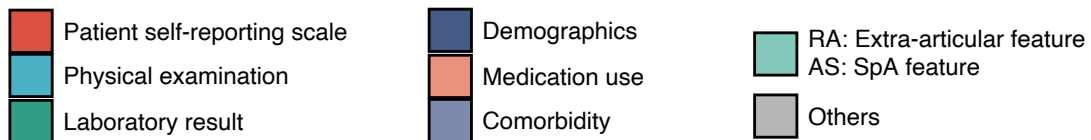
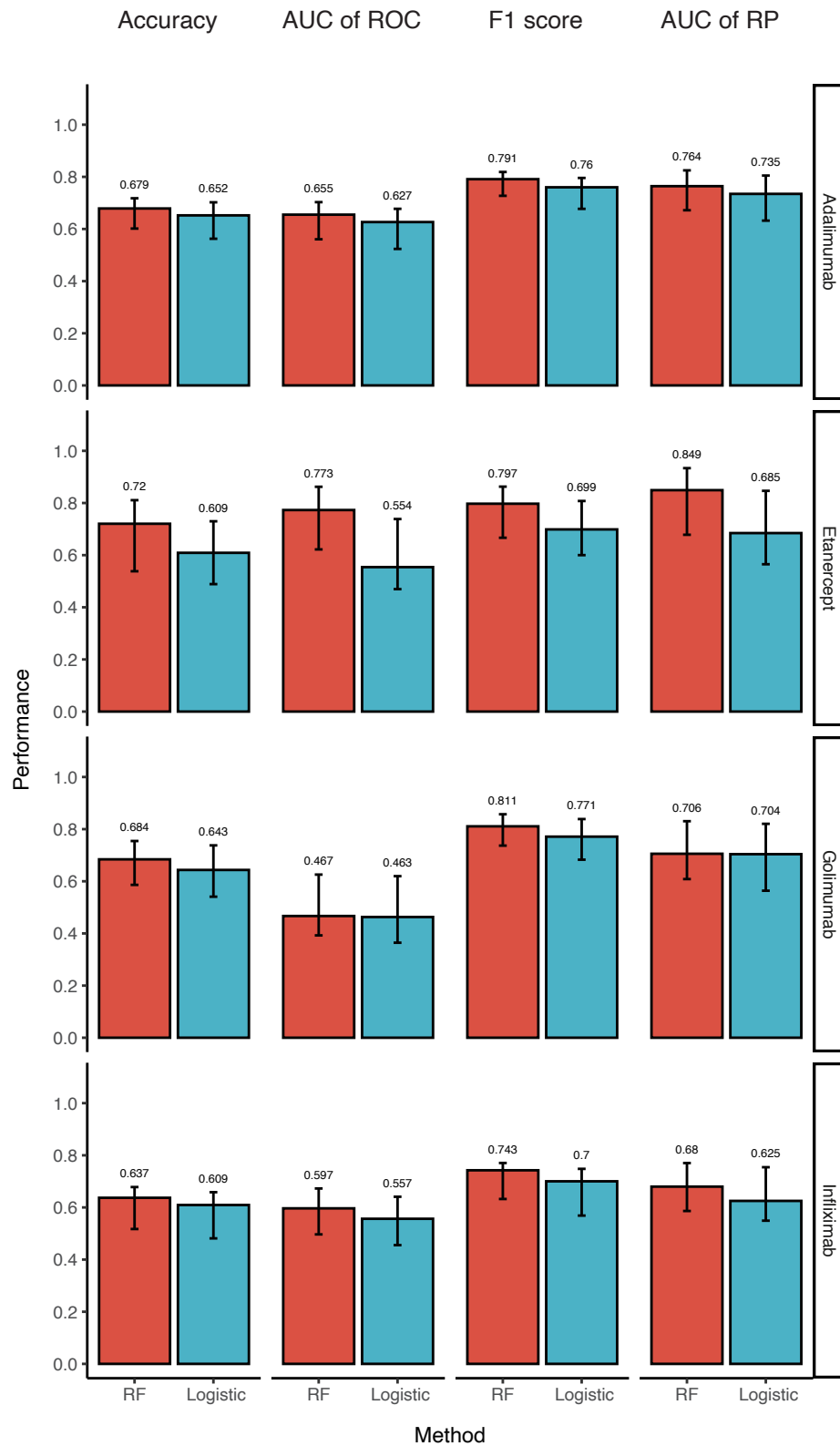


Figure S9. Performance of RF and logistic regression models in AS patients divided by the type of bDMARDs, (a) by training dataset, and (b) by independent test dataset.

(a)



(b)

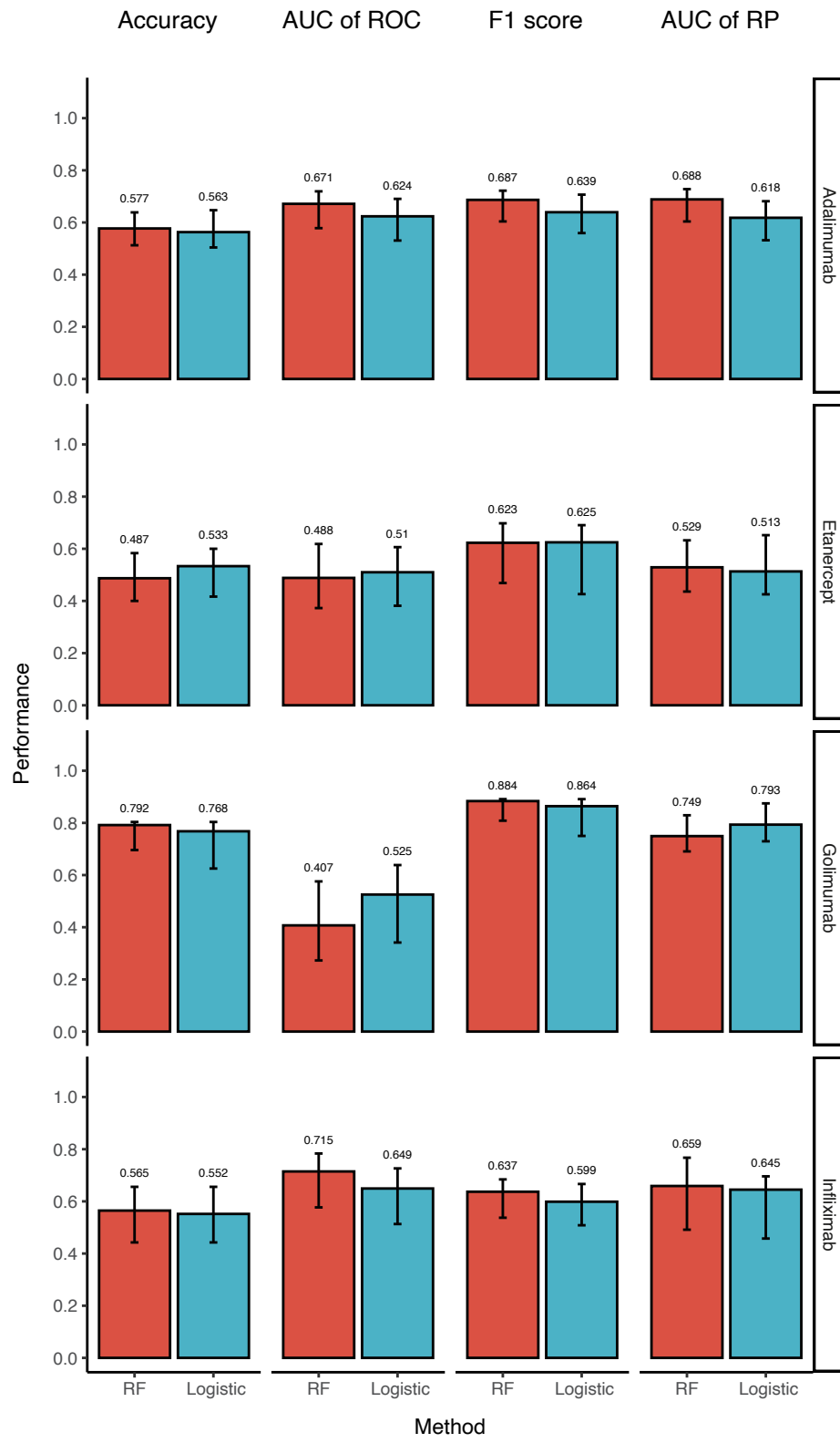
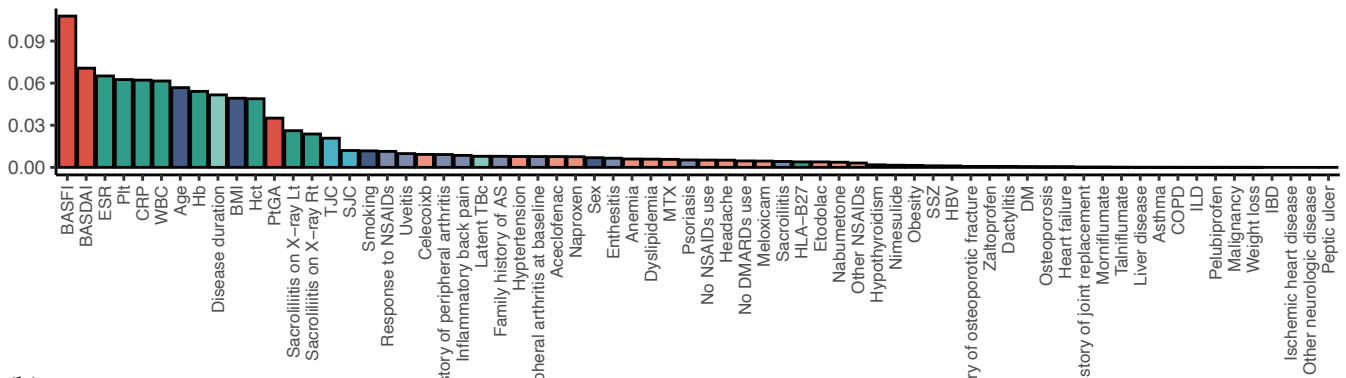
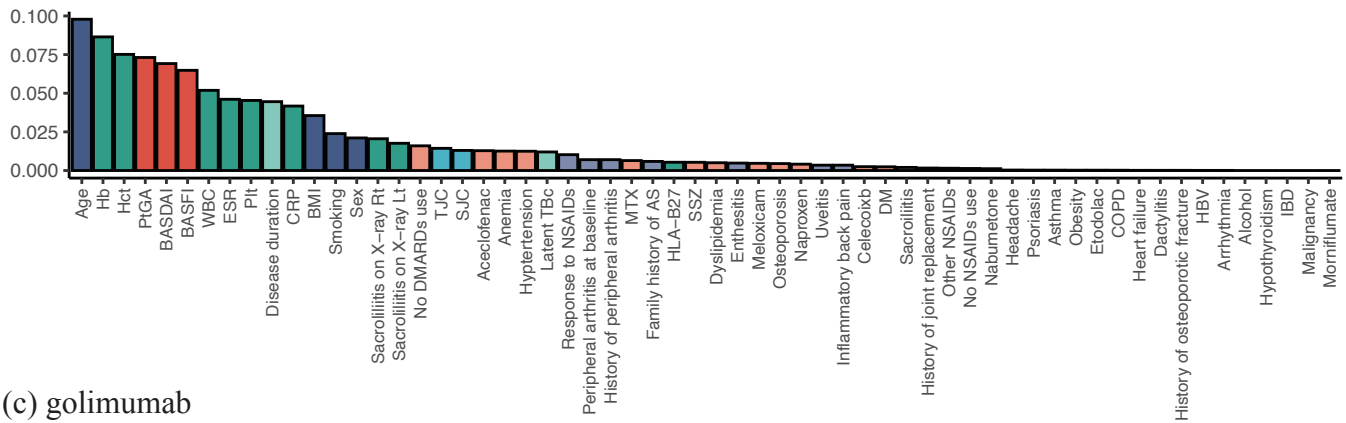


Figure S10. Feature importance analysis of the best-performing RF-method model in AS patients divided by the type of bDMARDs. (a) Adalimumab, (b) etanercept, (c) golimumab, and (d) infliximab.

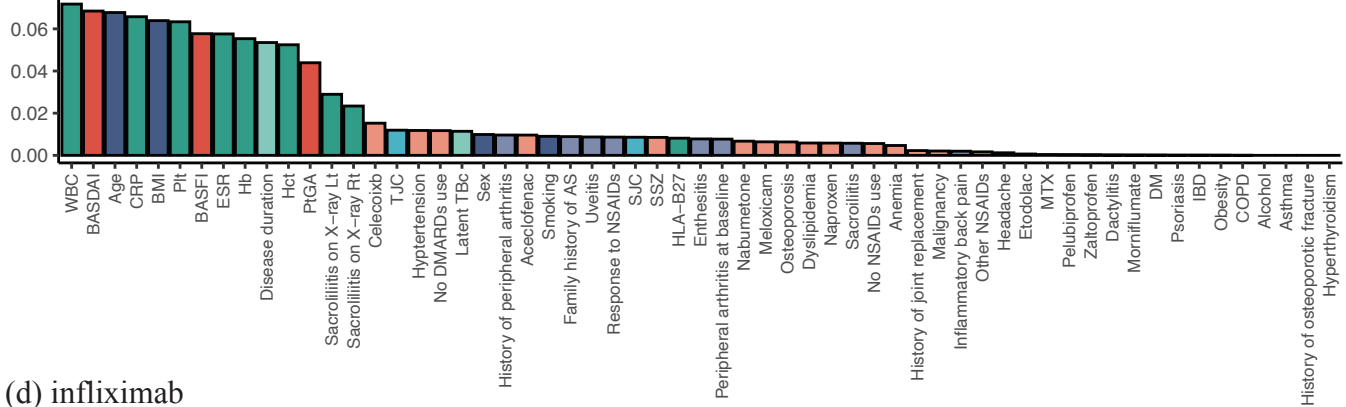
(a) adalimumab



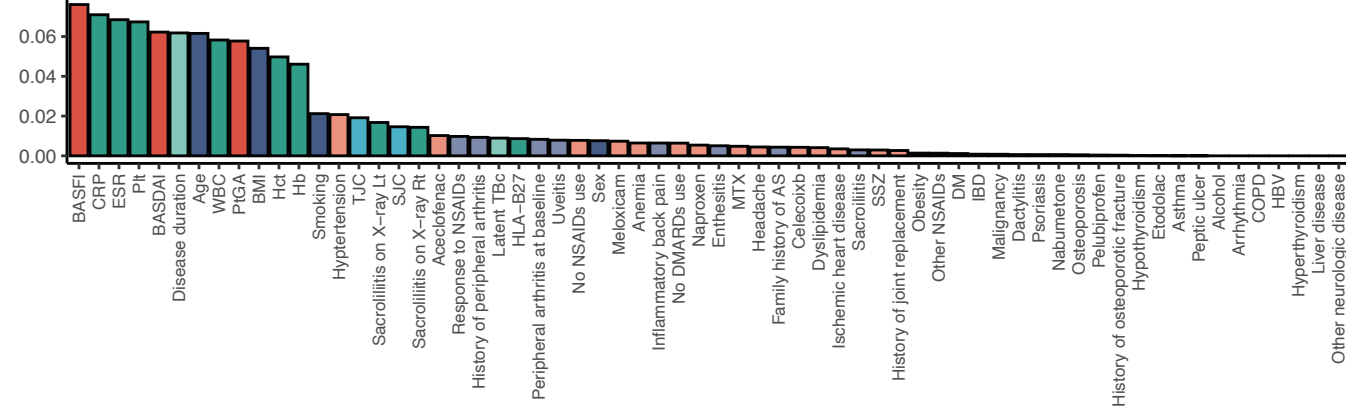
(b) etanercept



(c) golimumab



(d) infliximab



Category

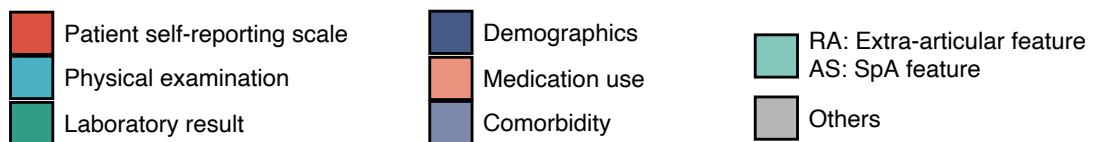
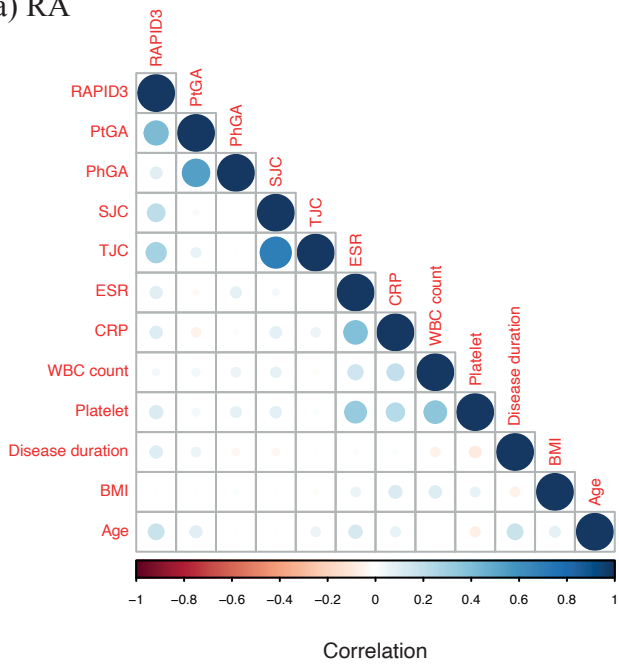


Figure S11. Correlation analysis between input features that reported the feature importance analysis. (a) RA, (b) AS.

(a) RA



(b) AS

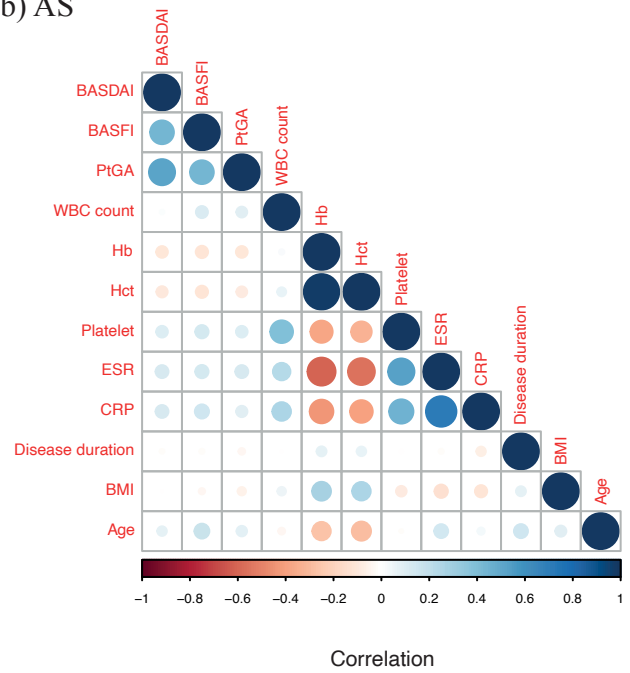
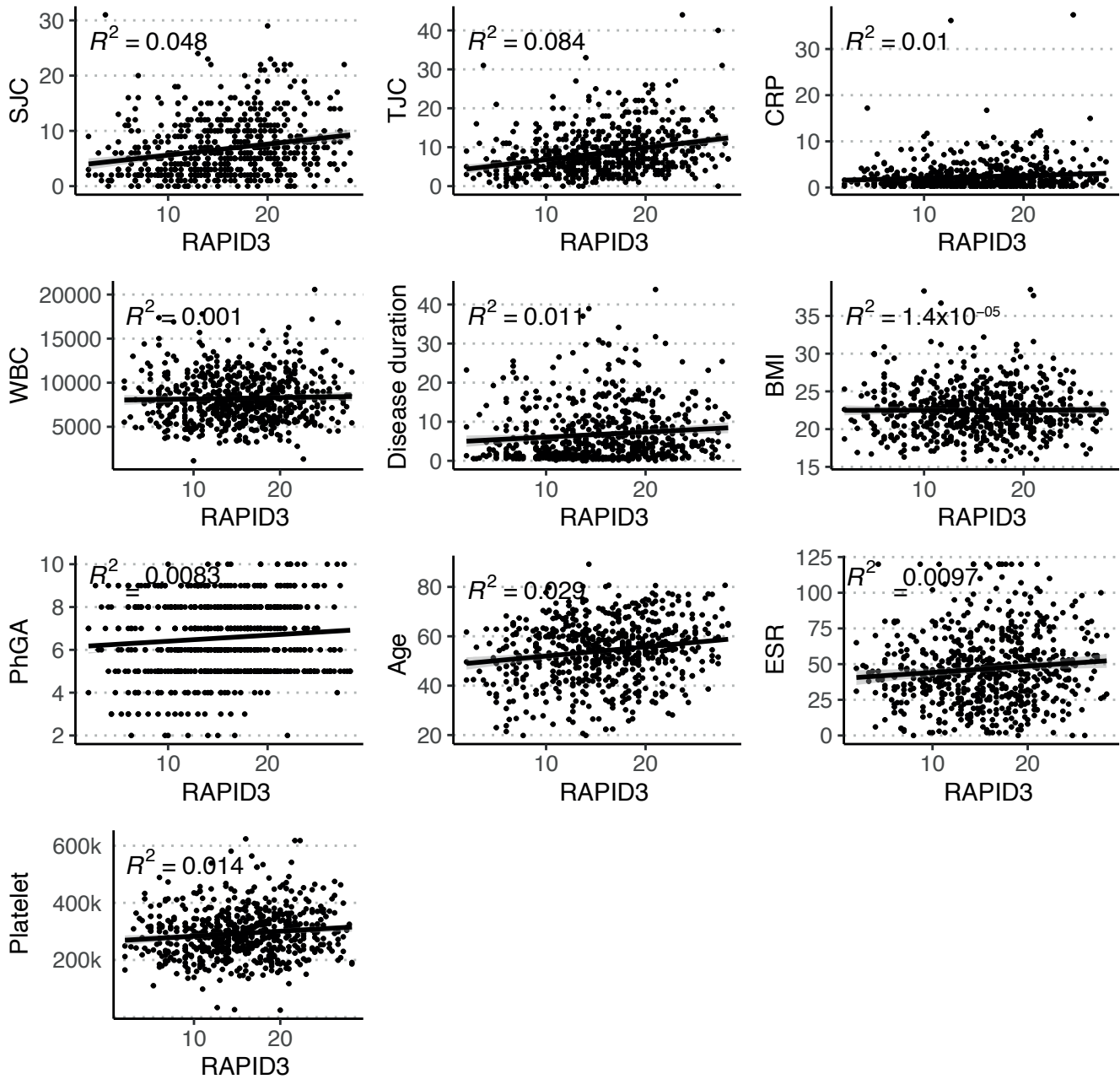
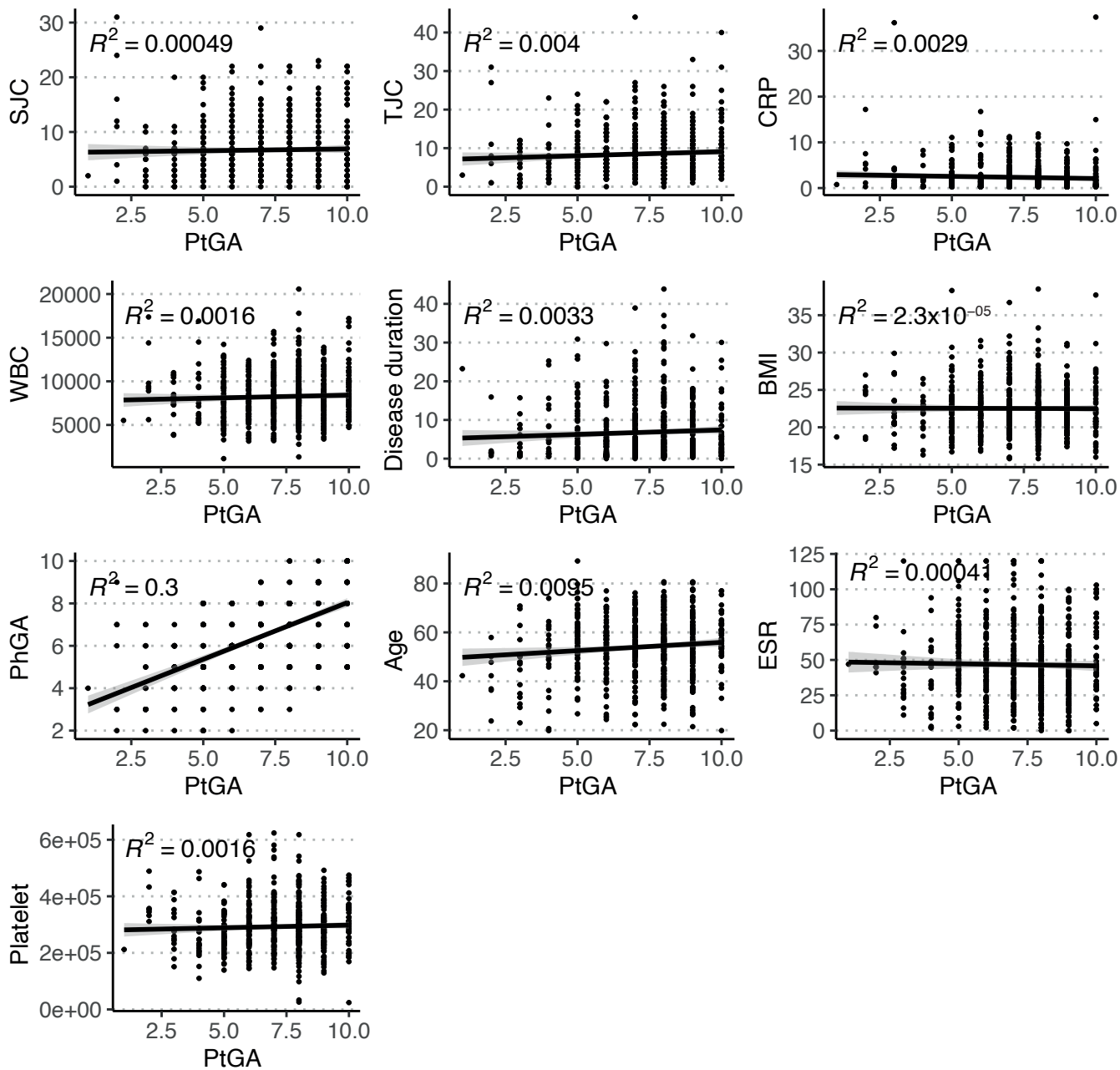


Figure S12. Linear regression analysis with dot plot results for (a) RAPID3 and other features, (b) PtGA and other features in patients with RA; between (c) BASFI and other features, (d) BASDAI and other features, (e) PtGA and other features in patients with AS; (f) between patient self-reporting scales in both diseases.

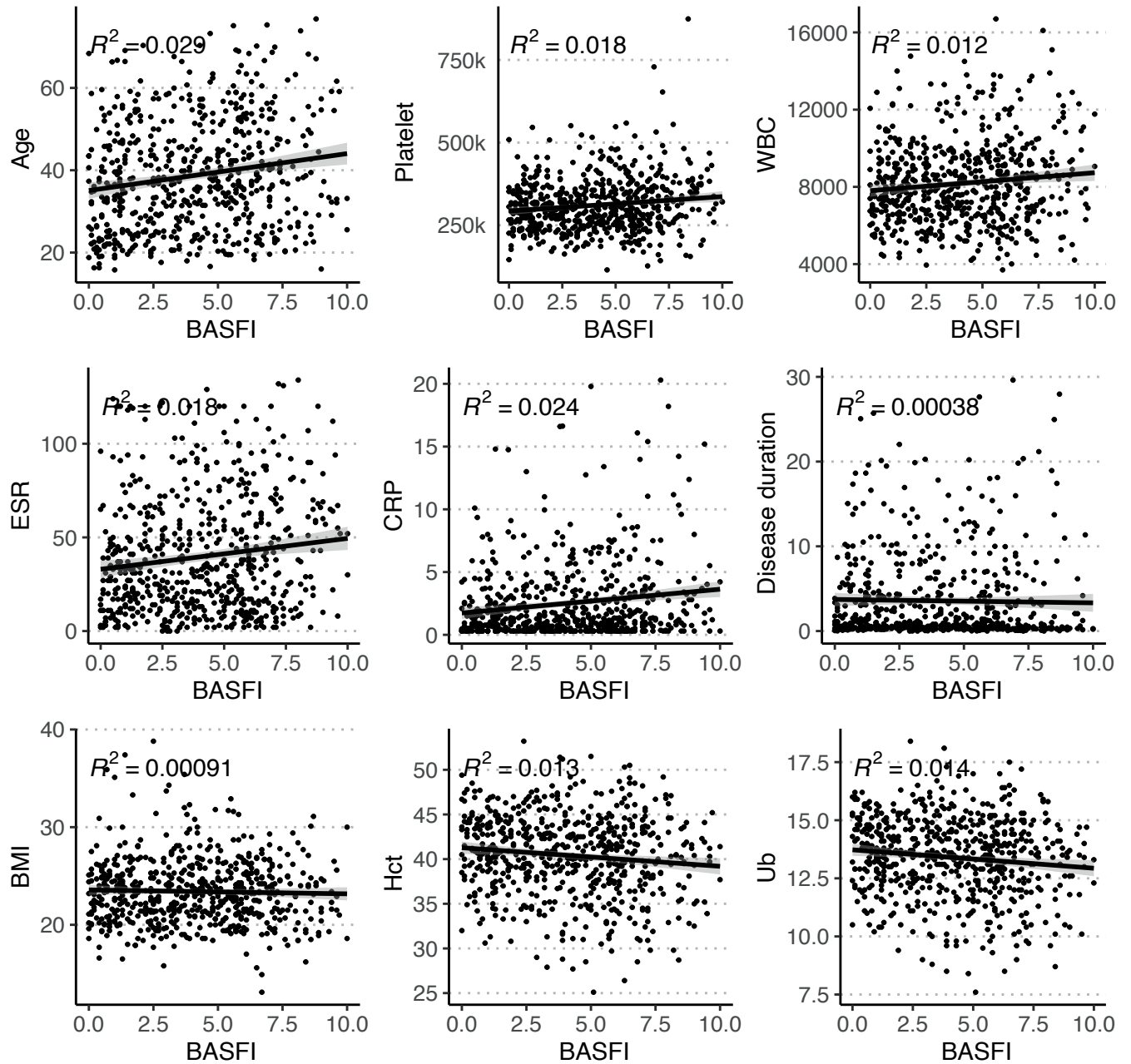
(a) RAPID3 and other features in patients with RA



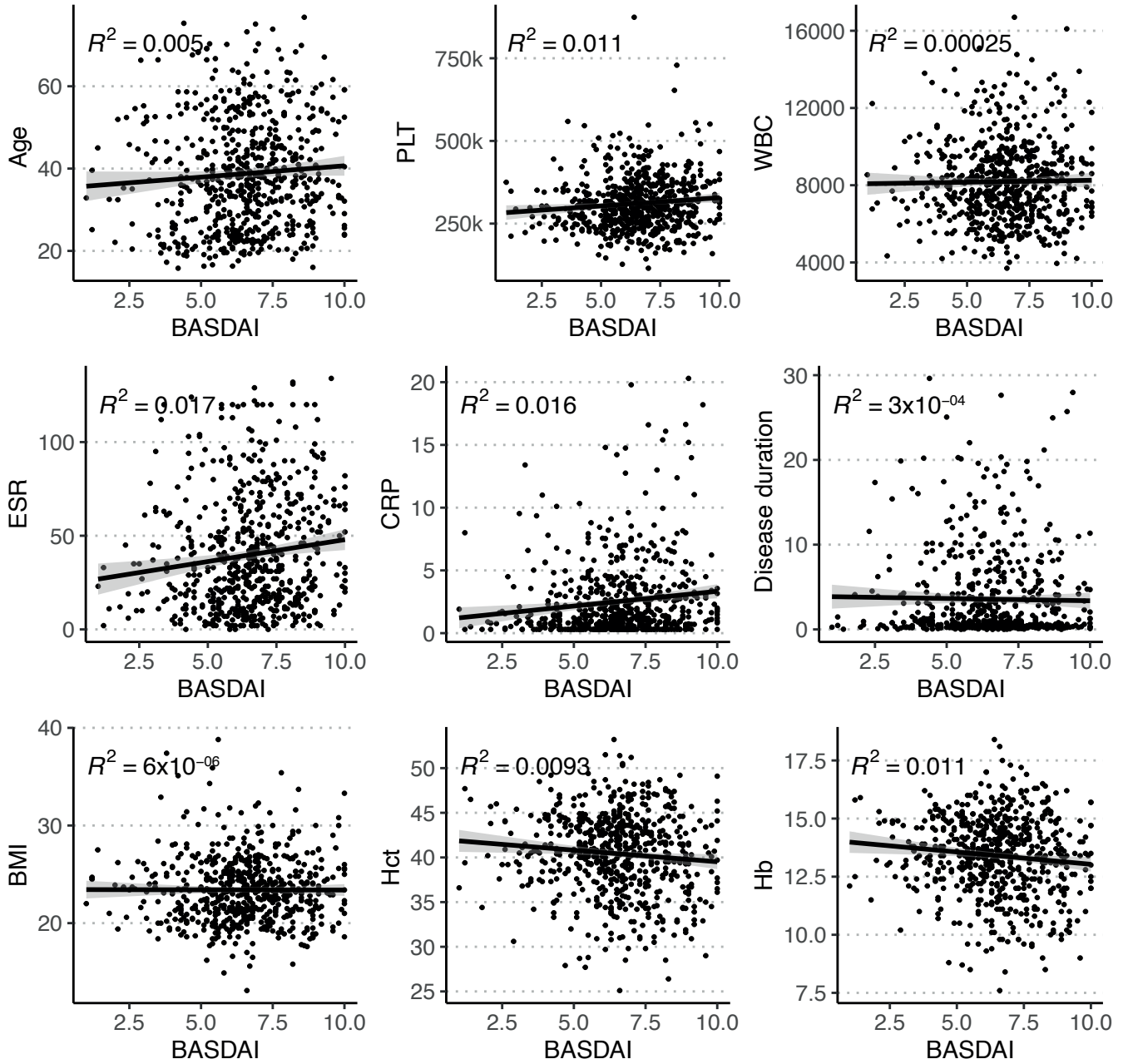
(b) PtGA and other features in patients with RA



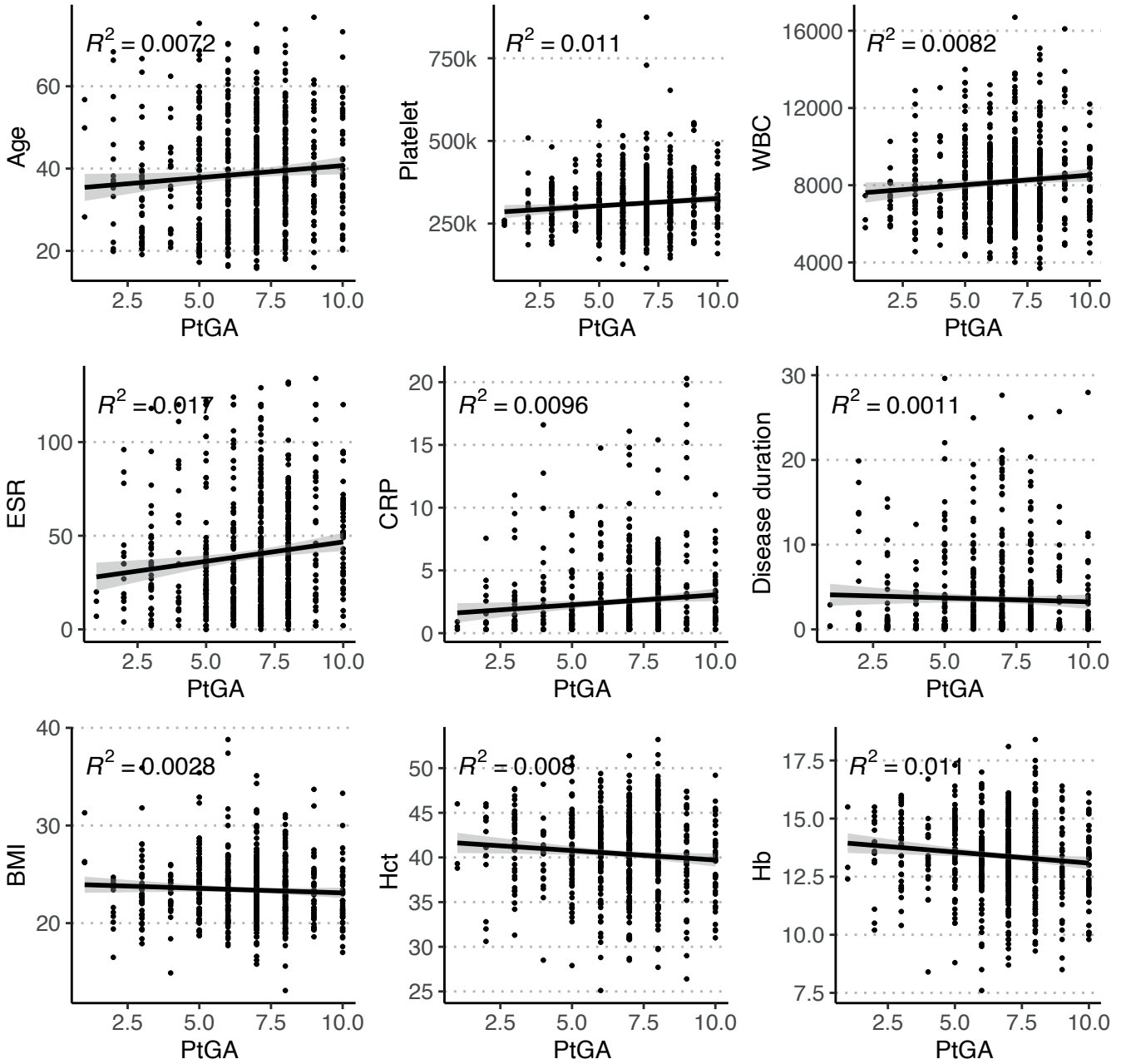
(c) BASFI and other features in patients with AS



(d) BASDAI and other features in patients with AS



(e) PtGA and other features in patients with AS



(f) between patient self-reporting scales in both diseases.

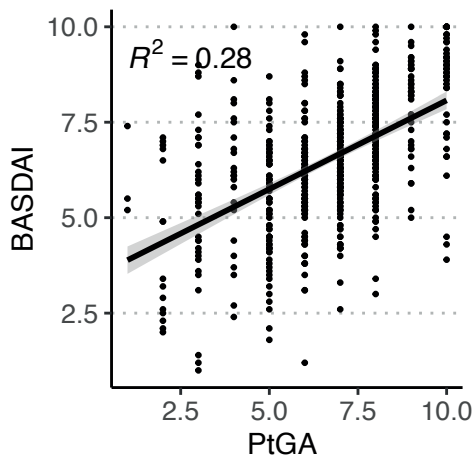
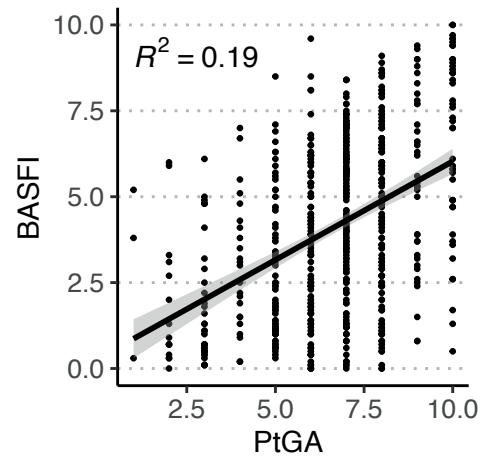
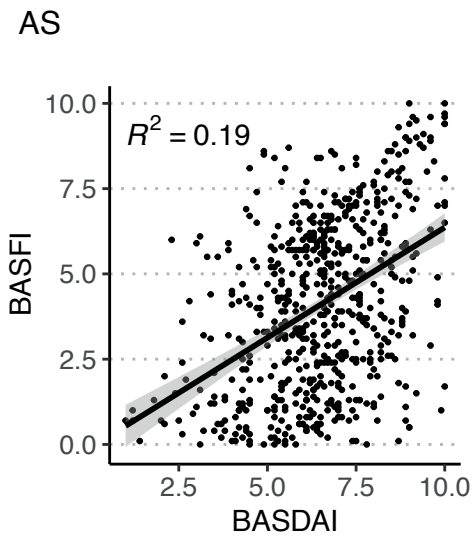
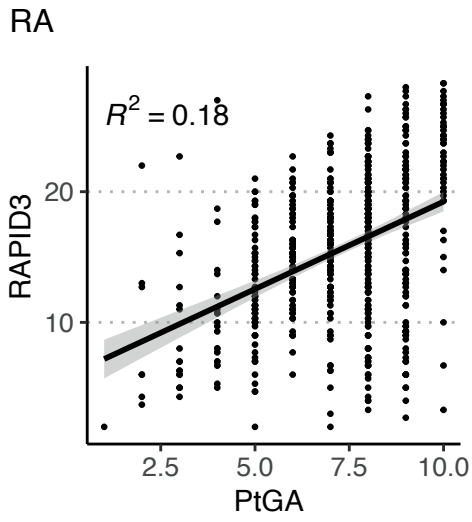
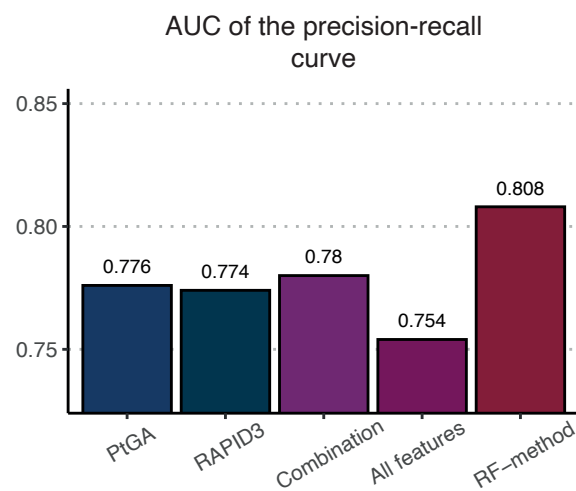
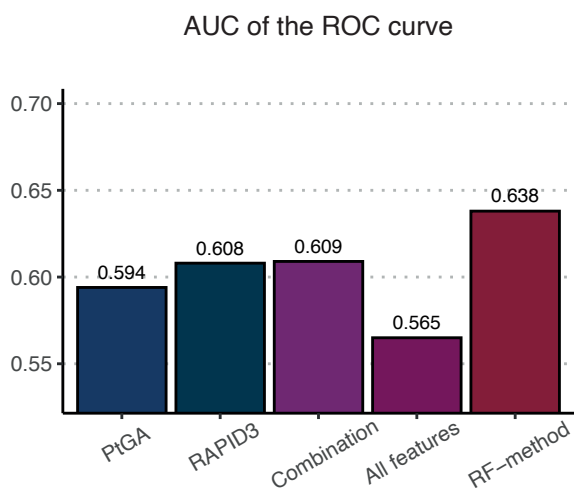


Figure S13. Prediction performances of logistic regression models using patient self-reported scales and their combinations. (a) RA, (b) AS.

(a) RA



(b) AS

